

# GLOBAL BIFURCATION DIAGRAMS OF POSITIVE SOLUTIONS FOR A CLASS OF 1-D SUPERLINEAR INDEFINITE PROBLEMS

M. FENCL AND J. LÓPEZ-GÓMEZ

**ABSTRACT.** This paper analyzes the structure of the set of positive solutions of a class of one-dimensional symmetric superlinear indefinite bvp's. It is a paradigm of how mathematical analysis aids the numerical study of a problem, whereas simultaneously its numerical study confirms and illuminates the analysis. On the analytical side, we establish the fast point-wise decay of the positive solutions as  $\lambda \downarrow -\infty$  in the region where  $a(x) < 0$  (see (1.1)), and solve positively the conjecture of [28] in two special cases of interest, where we show the existence of  $2^{n+1} - 1$  positive solutions for sufficiently negative  $\lambda$ . On the numerical side, this paper ascertains the global structure of the set of positive solutions on some paradigmatic prototypes whose intricate behavior is far from predictable from existing analytical results.

*2010 MSC:* 34B15, 34B08, 65N35, 65P30

*Keywords and phrases:* superlinear indefinite problems, positive solutions, bifurcation, uniqueness, multiplicity, global components, path-following, pseudo-spectral methods, finite-differences schemes.

Partially supported by the Research Grant PGC2018-097104-B-I00 of the Spanish Ministry of Science, Innovation and Universities, and the Institute of Inter-disciplinary Mathematics (IMI) of Complutense University. M. Fencl has been supported by the project SGS-2019-010 of the University of West Bohemia, the project 18-03253S of the Grant Agency of the Czech Republic and the project LO1506 of the Czech Ministry of Education, Youth and Sport.

## 1. INTRODUCTION

In this paper we study, analytically and numerically, the structure of the global bifurcation diagrams of positive solutions of the one-dimensional semilinear boundary value problem

$$\begin{cases} -u'' = \lambda u + a(x)u^2 & \text{in } (0, 1), \\ u(0) = u(1) = 0, \end{cases} \quad (1.1)$$

where  $a \in C[0, 1]$  is a real function that changes the sign in  $(0, 1)$  and  $\lambda \in \mathbb{R}$  is regarded as a bifurcation parameter. In our numerical experiments we have used the special choices

$$a(x) := \sin[(2n + 1)\pi x], \quad n \in \{1, 2, 3\}, \quad (1.2)$$

as well as

$$a(x) := \begin{cases} \mu \sin(5\pi x) & \text{if } x \in [0, 0.2) \cup (0.8, 1], \\ \sin(5\pi x) & \text{if } x \in [0.2, 0.8], \end{cases} \quad (1.3)$$

where  $\mu \geq 1$  is regarded as a secondary bifurcation parameter. These examples have  $n + 1$  positive and  $n$  negative bumps.

Since  $a(x)$  changes the sign, (1.1) is a superlinear indefinite problem. These problems have attracted a lot of attention during the last three decades. Some significant monographs dealing with them are those of H. Berestycki, I. Capuzzo-Dolcetta and L. Nirenberg [5, 6], S. Alama and G. Tarantello [1], H. Amann and J. López-Gómez [3], R. Gómez-Reñasco and J. López-Gómez [28, 29], J. Mawhin, D. Papini and F. Zanolin [59], J. López-Gómez, A. Tellini and F. Zanolin [56], J. López-Gómez and A. Tellini [55], G. Feltrin and F. Zanolin, as well

as Chapter 9 of J. López-Gómez [41], the recent monograph of G. Feltrin [23], and the list of references there in. Superlinear indefinite problems have been recently introduced in the context of quasilinear elliptic equations by J. López-Gómez, P. Omari and S. Rivetti [53, 54], and J. López-Gómez and P. Omari [50, 51, 52].

Thanks to H. Amann and J. López-Gómez [3], it is already known that (1.1) possesses a component of positive solutions,  $\mathcal{C}^+ \subset \mathbb{R} \times \mathcal{C}[0, 1]$ , such that  $(\pi^2, 0) \in \mathcal{C}^+$ , i.e.,  $\mathcal{C}^+$  bifurcates from  $u = 0$  at  $\lambda = \pi^2$ . Note that  $\lambda = \pi^2$  is the lowest eigenvalue of  $-D^2$  in  $(0, 1)$  under homogeneous Dirichlet boundary conditions. Moreover, the component  $\mathcal{C}^+$  is unbounded in  $\mathbb{R} \times \mathcal{C}[0, 1]$ , and (1.1) cannot admit a positive solution for sufficiently large  $\lambda > \pi^2$ . Furthermore, by the existence of universal a priori bounds, uniform on compact subintervals of  $\lambda \in \mathbb{R}$ , for the positive solutions of (1.1), it is apparent that  $(-\infty, \pi^2) \subset \mathcal{P}_\lambda(\mathcal{C}^+)$ , where  $\mathcal{P}_\lambda$  stands for the  $\lambda$ -projection operator defined by

$$\mathcal{P}_\lambda(\lambda, u) = \lambda, \quad (\lambda, u) \in \mathbb{R} \times \mathcal{C}[0, 1].$$

Actually, according to R. Gómez-Reñasco and J. López-Gómez [28, 29], either  $\mathcal{P}_\lambda(\mathcal{C}^+) = (-\infty, \pi^2)$ , or there exists  $\lambda_t > \pi^2$  such that  $\mathcal{P}_\lambda(\mathcal{C}^+) = (-\infty, \lambda_t]$ . Moreover, (1.1) admits some stable positive solution if, and only if,  $\lambda \in (\pi^2, \lambda_t]$ , and, in such case, the stable solution is unique, and it equals the minimal positive solution of (1.1). The fact that  $\lambda_t$  is turning point is emphasized by its subindex.

Besides the (optimal) multiplicity result of H. Amann and J. López-Gómez [3], establishing that (1.1) has, at least, two positive solutions for every  $\lambda \in (\pi^2, \lambda_t)$  if  $\lambda_t > \pi^2$ , there are some others multiplicity results by M. Gaudenzi, P. Habets and F. Zanolin [27] later generalized by G. Feltrin and F. Zanolin [24] and G. Feltrin [23]. Precisely, according to Corollary 1.4.2 of G. Feltrin [23], which extends [27, Th.2.1], setting  $a = a^+ - \mu a^-$ , there exists  $\mu_c > 0$  such that, for every  $\mu > \mu_c$ , the problem

$$\begin{cases} -u'' = (a^+ - \mu a^-)u^2 & \text{in } (0, 1), \\ u(0) = u(1) = 0, \end{cases} \quad (1.4)$$

possesses, for every  $\mu > \mu_c$ , at least,  $2^{n+1} - 1$  positive solutions if  $a(x)$  is given by (1.2). However, this result does not solve the conjecture of R. Gómez-Reñasco and J. López-Gómez [28] according with it there exists  $\lambda_c < \pi^2$  such that, for every  $\lambda < \lambda_c$ , the problem (1.1) possesses, at least,

$$\sum_{j=1}^{n+1} \binom{n+1}{j} = 2^{n+1} - 1$$

positive solutions; among them,  $n + 1$  with a single peak around each of the maxima of  $a(x)$ ,  $\frac{(n+1)n}{2}$  with two peaks, and, in general,  $\frac{(n+1)!}{j!(n+1-j)!}$  with  $j$  peaks for every  $j \in \{1, \dots, n + 1\}$ . For instance, when  $n = 1$ , then  $a(x) = \sin(3\pi x)$  and, according to our numerical experiments, (1.1) indeed has, for sufficiently negative  $\lambda$ , three positive solutions: one with a bump on the left, one with a bump on the right, and another one with two bumps (see Figure 3a). Note that, essentially, Corollary 1.4.2 of G. Feltrin [23] establishes that (1.1) possesses  $2^{n+1} - 1$  positive solutions provided  $\lambda = 0$  and  $\|a^-\|_\infty$  is sufficiently large, though it does not give any information for  $\lambda < 0$ . Thus, the conjecture of [28] seems to remain open after two decades.

The main goal of this paper is to deliver a proof of this conjecture in some special cases of interest, with  $a(x)$  is symmetric about 0.5, as well as to complete systematically some of the old numerical experiments of R. Gómez-Reñasco and J. López-Gómez [28, 30] to gain insight into the most ambitious problem of ascertaining the global topological structure of the set of positive solutions of (1.1). In this paper we complete, both analytically and numerically, some

of the previous findings of [28, 30, 41] for the special cases when  $n = 1$  and  $n = 2$ . As a direct consequence of our numerical experiments for the special choice (1.3), it becomes apparent the optimality of [23, Cor. 1.4.2], in the sense that, for sufficiently small  $\mu$ , the problem (1.4) might have less than  $2^{n+1} - 1$  positive solutions.

The organization of this paper is the following. In Section 2 we collect the available information concerning the global structure of the set of positive solutions of (1.1). In Section 3 we show that, for every family of positive solutions of (1.1),  $\{(\lambda, u_\lambda)\}_{\lambda < 0}$ , one has that

$$\lim_{\lambda \downarrow -\infty} u_\lambda(x) = 0 \quad \text{for all } x \in \Omega_- = \text{int supp } a^-, \quad (1.5)$$

uniformly on compact subsets of  $\Omega_-$ . Then, this result is used to establish the validity of the conjecture of [28] in the special, but important, case when  $a$  is symmetric about 0.5 and  $a^+$  is piecewise constant. Actually, the same proof also shows the validity of the multiplicity result when  $a(x)$  is given by either (1.2), or (1.3), provided the associated homogeneous Dirichlet boundary value problem on each of the components where  $a > 0$  admit a symmetric positive solution with a single peak at its middle point, which is greatly confirmed by all our numerical experiments. In Sections 4, 5 and 6 we provide with the results of our numerical experiments in cases  $n = 1$ ,  $n = 2$  and  $n = 3$ , respectively. In Section 7 we analyze the more sophisticated case when  $a$  is given by (1.3) using  $\mu \geq 1$  as the secondary bifurcation parameter. In Section 8 we discuss the necessary numerics to implement all the numerical experiments of this paper. The paper ends with the final discussion carried out in Section 9.

Actually, Theorem 3.1 supports the conjecture of [28] in the general case, because it establishes that the positive solutions of (1.1) should be perturbations of a family of  $2^{n+1} - 1$  weak positive subsolutions of (1.1). Indeed, suppose that

$$\text{supp } a^+ = \bigcup_{j=1}^{n+1} I_j^+ \quad \text{and} \quad \text{supp } a^- = \bigcup_{j=1}^n I_j^-,$$

where the  $I_j^+$ 's and the  $I_i^-$ 's are compact nontrivial intervals such that  $I_i^-$  is separated by  $I_i^+$  and  $I_{i+1}^+$  for every  $i \in \{1, \dots, n\}$ , and  $I_j^+ \equiv [\alpha_j, \beta_j]$ ,  $j \in \{1, \dots, n+1\}$ . For every  $j \in \{1, \dots, n+1\}$ , let  $\theta_{\{\lambda, j\}}$  be any positive solution of

$$\begin{cases} -u'' = \lambda u + a^+(x)u^2 & \text{in } (\alpha_j, \beta_j), \\ u(\alpha_j) = u(\beta_j) = 0. \end{cases} \quad (1.6)$$

This solution exists by the theory of H. Amann and J. López-Gómez [3]. Next, for every set of  $n + 1$  digits  $d_j \in \{0, 1\}$ ,  $1 \leq j \leq n + 1$ , such that  $d_j = 1$  for some  $j \in \{1, \dots, n + 1\}$ , we consider

$$T \equiv d_1 d_2 d_3 \cdots d_{n+1} \equiv (d_1, d_2, d_3, \dots, d_{n+1})$$

as well as the weak subsolution of (1.1) defined through

$$\Theta_T := \begin{cases} d_j \theta_{\{\lambda, j\}} & \text{in } I_j^+, \quad j \in \{1, \dots, n+1\}, \\ 0 & \text{in } I_i^-, \quad i \in \{1, \dots, n\}. \end{cases}$$

Should each of these solutions perturb into a positive solution of (1.1), as it is rather natural at the light of (1.5), it becomes apparent that (1.1) should admit, at least,  $2^{n+1} - 1$  positive solutions for sufficiently negative  $\lambda$ . In this case,  $T$  is referred to as the *type* of such a solution. Throughout this paper, we use this convention for representing the positive solutions of (1.1). Thus, for any  $a(x)$  with  $n + 1$  positive bumps separated away by negative ones, we use a code with  $n + 1$  digits in  $\{0, 1\}$ , where 1 means that the solution has a bump localized at the maximum indicated by its position in the code, whereas 0 means that no bump in that

position exists. Thus, when, e.g.,  $a(x) = \sin(3\pi x)$ , we have positive solutions in Figure 3a represented by 2-digit codes, where 00 stands for the trivial solution, 10 stands for a solution with a single bump on the left, 01 stands for a solution with one single bump on the right, and 11 stands for a positive solution with both bumps around each of the interior maxima of  $a(x)$ . At the end of this code, called the *type of the solution* in this paper, we will always add a positive integer within parenthesis, the *Morse index*, i.e., the dimension of the unstable manifold of the positive solution as a steady state of the associated parabolic problem

$$\begin{cases} \frac{\partial u}{\partial t} - \frac{\partial^2 u}{\partial x^2} = \lambda u + a(x)u^2, & t > 0, \quad x \in (0, 1), \\ u(0, t) = u(1, t) = 0, & t > 0, \\ u(x, 0) = u_0(x), & x \in [0, 1], \end{cases} \quad (1.7)$$

where  $u_0$  is the initial data. The dimension of the unstable manifold of a given steady state solution, say  $u$ , equals the number of negative eigenvalues,  $\tau$ , of the linearized problem

$$\begin{cases} -v'' = \lambda v + 2a(x)u(x)v + \tau v & \text{in } (0, 1), \\ v(0) = v(1) = 0. \end{cases} \quad (1.8)$$

## 2. GLOBAL STRUCTURE OF THE COMPONENT $\mathcal{C}^+$

This section analyzes the local and global behaviors of the component of positive solutions  $\mathcal{C}^+$  introduced in Section 1. The next result, of a technical nature, allows us to express, equivalently, (1.1) as a fixed point equation for a compact operator. As the proof is elementary, we omit it herein.

**Lemma 2.1.** *For every  $f \in \mathcal{C}[0, 1]$ , the function*

$$u(x) = \int_0^x (s-x)f(s) ds - x \int_0^1 (s-1)f(s) ds \quad (2.1)$$

*provides us with the unique solution of the linear boundary value problem*

$$\begin{cases} -u'' = f & \text{in } [0, 1], \\ u(0) = u(1) = 0. \end{cases} \quad (2.2)$$

According to Lemma 2.1, we introduce the linear integral operator  $K : \mathcal{C}[0, 1] \rightarrow \mathcal{C}^2[0, 1]$  defined, for every  $f \in \mathcal{C}[0, 1]$ , by

$$Kf(x) := \int_0^x (s-x)f(s) ds - x \int_0^1 (s-1)f(s) ds, \quad x \in [0, 1]. \quad (2.3)$$

Subsequently, for every integer  $n \geq 0$ , we denote by  $\mathcal{C}_0^n[0, 1]$  the closed subspace of the real Banach space  $\mathcal{C}^n[0, 1]$  consisting of all functions  $u \in \mathcal{C}^n[0, 1]$  such that  $u(0) = u(1) = 0$ , and denote  $\mathcal{C}[0, 1] := \mathcal{C}^0[0, 1]$ ,  $\mathcal{C}_0[0, 1] := \mathcal{C}_0^0[0, 1]$ . The next result collects a pivotal property of the integral operator  $K$ .

**Lemma 2.2.**  *$K : \mathcal{C}[0, 1] \rightarrow \mathcal{C}_0^2[0, 1]$  is linear and continuous.*

**Proof:** As the integral is linear,  $K$  is linear. Moreover, setting  $u := Kf$ , we have that

$$u'(x) = - \int_0^x f(s) ds - \int_0^1 (s-1)f(s) ds \quad \text{and} \quad u''(x) = -f(x)$$

for all  $x \in [0, 1]$ . Thus,

$$\|u\|_\infty \leq 3\|f\|_\infty, \quad \|u'\|_\infty \leq 2\|f\|_\infty, \quad \|u''\|_\infty \leq \|f\|_\infty.$$

Therefore, for every  $f \in \mathcal{C}[0, 1]$ ,

$$\|Kf\|_{\mathcal{C}^2[0,1]} \leq 6\|f\|_\infty,$$

which ends the proof.  $\square$

Subsequently, we consider the canonical injection

$$j : \mathcal{C}_0^2[0, 1] \hookrightarrow \mathcal{C}_0^1[0, 1]. \quad (2.4)$$

Thanks to the Ascoli–Arzelà theorem, it is a linear compact operator. Thus,

$$\mathcal{K} := jK|_{\mathcal{C}_0^1[0,1]} : \mathcal{C}_0^1[0, 1] \rightarrow \mathcal{C}_0^1[0, 1], \quad (2.5)$$

also is a linear compact operator. Using  $\mathcal{K}$ , the problem (1.1) can be expressed as a fixed point equation for a compact operator, because  $u$  solves (1.1) if, and only if,

$$u = \mathcal{K}(\lambda u + au^2).$$

Note that  $R[\mathcal{K}] \subset \mathcal{C}_0^2[0, 1]$ , by the definition of  $\mathcal{K}$ . Thus, the solutions of (1.1) are the zeroes of the nonlinear operator  $\mathfrak{F} : \mathbb{R} \times \mathcal{C}_0^1[0, 1] \rightarrow \mathcal{C}_0^1[0, 1]$  defined by

$$\mathfrak{F}(\lambda, u) := u - \mathcal{K}(\lambda u + au^2), \quad (\lambda, u) \in \mathbb{R} \times \mathcal{C}_0^1[0, 1]. \quad (2.6)$$

Setting

$$\mathfrak{L}(\lambda)u := u - \lambda \mathcal{K}u, \quad \mathfrak{N}(\lambda, u) := -\mathcal{K}(au^2), \quad (\lambda, u) \in \mathbb{R} \times \mathcal{C}_0^1[0, 1], \quad (2.7)$$

it is apparent that

$$\mathfrak{F}(\lambda, u) = \mathfrak{L}(\lambda)u + \mathfrak{N}(\lambda, u)$$

satisfies the general structural requirements of Chapters 2 and 6 of [38], because  $\mathfrak{L}(\lambda)$  is an analytic compact perturbation of the identity map on  $\mathcal{C}_0^1[0, 1]$ ,  $I$ , and the nonlinearity is completely continuous, i.e., continuous and compact, and, being a polynomial, also is analytic. In particular,  $\mathfrak{L}(\lambda)$  is Fredholm of index zero for all  $\lambda \in \mathbb{R}$ , and  $\mathfrak{F}$  is a compact perturbation of the identity map that it is real analytic in  $(\lambda, u) \in \mathbb{R} \times \mathcal{C}_0^1[0, 1]$ . Thus, the main theorems of M. G. Crandall and P. H. Rabinowitz [15, 16], as well as the unilateral global bifurcation theorem of López-Gómez [38, Th. 6.4.3], can be applied.

The generalized spectrum,  $\Sigma(\mathfrak{L})$ , of the Fredholm curve  $\mathfrak{L}(\lambda)$  defined in (2.7) consists of the set of  $\lambda \in \mathbb{R}$  for which  $u = \lambda \mathcal{K}u$  for some  $u \in \mathcal{C}_0^1[0, 1]$ ,  $u \neq 0$ . Differentiating twice with respect to  $x$ , this fixed point equation can be equivalently expressed as

$$\begin{cases} -u'' = \lambda u & \text{in } [0, 1], \\ u(0) = u(1) = 0. \end{cases} \quad (2.8)$$

Thus,

$$\Sigma(\mathfrak{L}) = \left\{ \sigma_n \equiv (n\pi)^2 : n \in \mathbb{N}, n \geq 1 \right\}.$$

Moreover,

$$N[\mathfrak{L}(\lambda_n)] = \text{span}[\psi_n], \quad \psi_n(x) = \sin(n\pi x), \quad x \in [0, 1].$$

Subsequently, in order to apply the main theorem of [15] at  $\sigma_n = (n\pi)^2$ , we fix  $n \geq 1$  and, adopting the notations of [38, Ch. 2], we set  $(\lambda_0, \varphi_0) \equiv (\sigma_n, \psi_n)$ . Then,

$$N[\mathfrak{L}_0] = \text{span}[\varphi_0], \quad \mathfrak{L}_0 \equiv \mathfrak{L}(\lambda_0) = I - \sigma_n \mathcal{K}, \quad \mathfrak{L}_1 \equiv \mathfrak{L}'(\lambda_0) = -\mathcal{K},$$

and the following transversality condition holds

$$\mathfrak{L}_1(N[\mathfrak{L}_0]) \oplus R[\mathfrak{L}_0] = \mathcal{C}_0^1[0, 1]. \quad (2.9)$$

On the contrary, assume that  $\mathfrak{L}_1\varphi_0 \in R[\mathfrak{L}_0]$ . Then, there exists  $u \in \mathcal{C}_0^1[0, 1]$  such that

$$-\mathcal{K}\varphi_0 = \mathfrak{L}_1\varphi_0 = \mathfrak{L}_0u = u - \sigma_n \mathcal{K}u$$

and hence, differentiating twice with respect to  $x$ , it becomes apparent that

$$-\varphi_0 = -u'' - \sigma_n u.$$

Consequently, multiplying by  $\varphi_0$  and integrating in  $(0, 1)$  yields

$$-\int_0^1 \varphi_0^2 dx = \int_0^1 [(-u'' - \sigma_n u)\varphi_0] dx = \int_0^1 [(-\varphi_0'' - \sigma_n \varphi_0)u] dx = 0,$$

which is impossible. This shows (2.9). Therefore, as a direct application of the main theorem of M. G. Crandall and P. H. Rabinowitz [15], the following result of a local nature holds.

**Theorem 2.1.** *For any given integer  $n \geq 1$ , let  $Y$  denote the closed subspace of  $\mathcal{C}_0^1[0, 1]$  defined by*

$$Y := \left\{ w \in \mathcal{C}_0^1[0, 1] : \int_0^1 w(x)\psi_n(x) dx = 0 \right\}.$$

*Then, there exist  $\eta > 0$  and two analytic maps  $\lambda_n : (-\eta, \eta) \rightarrow \mathbb{R}$  and  $y_n : (-\eta, \eta) \rightarrow Y$  such that*

- $\lambda_n(0) = \sigma_n$ ,  $y_n(0) = 0$ ;
- $\mathfrak{F}(\lambda_n(s), s(\psi_n + y_n(s))) = 0$  for all  $s \in (-\eta, \eta)$ ; and
- *the solutions of the curve  $(\lambda_n(s), s(\psi_n + y_n(s)))$ ,  $|s| < \eta$ , are the unique zeroes of  $\mathfrak{F}$ , besides  $(\lambda, 0)$ , in a neighborhood of  $(\sigma_n, 0)$  in  $\mathbb{R} \times \mathcal{C}_0^1[0, 1]$ .*

Since  $y_n(0) = 0$ , the function  $u(s) = s(\psi_n + y_n(s)) \in \mathcal{C}_0^2[0, 1]$  has the same nodal behavior as  $\psi_n$  for sufficiently small  $s \neq 0$ , because  $y_n(s) \sim 0$  in  $\mathcal{C}_0^1[0, 1]$  and the zeroes of  $\psi_n$  are simple. Therefore, by Theorem 2.1, it is apparent that, for every  $n \geq 1$ , (1.1) has a curve of solutions with  $n - 1$  zeroes bifurcating from  $u = 0$  at  $\lambda = \sigma_n$ , regardless the nature of the weight function  $a \in \mathcal{C}[0, 1]$ . In particular, by the local uniqueness result at  $(\sigma_n, 0)$ , the positive solution of (1.1) can only bifurcate from  $u = 0$  at the critical value of the parameter  $\sigma_1 = \pi^2$ . Next, we will analyze the local nature of this bifurcation from  $(\lambda, u) = (\sigma_1, 0)$ . Setting  $D_1 := \lambda_1'(0)$ ,  $D_2 := \lambda_1''(0)$ ,  $w_1 := y_1'(0)$  and  $w_2 := y_1''(0)$ , we have that

$$\lambda_1(s) = \sigma_1 + sD_1 + s^2D_2 + O(s^3), \quad y_1(s) = sw_1 + s^2w_2 + O(s^3),$$

as  $s \rightarrow 0$ . By Theorem 2.1, we already know that

$$\begin{aligned} -s(\psi_1 + sw_1 + s^2w_2 + O(s^3))'' &= [\sigma_1 + sD_1 + s^2D_2 + O(s^3)] \\ &\quad + a(x)s(\psi_1 + sw_1 + s^2w_2 + O(s^3))s(\psi_1 + sw_1 + s^2w_2 + O(s^3)) \end{aligned}$$

for  $s \simeq 0$ . Thus, dividing by  $s$  yields

$$\begin{aligned} -(\psi_1 + sw_1 + s^2w_2 + O(s^3))'' &= [\sigma_1 + sD_1 + s^2D_2 + O(s^3)] \\ &\quad + a(x)s(\psi_1 + sw_1 + s^2w_2 + O(s^3))(\psi_1 + sw_1 + s^2w_2 + O(s^3)). \end{aligned} \quad (2.10)$$

Particularizing (2.10) at  $s = 0$ , yields to  $-\psi_1'' = \sigma_1\psi_1$ , which holds true by the definition of  $\psi_1$ . Identifying terms of the first order in  $s$ , it follows from (2.10) that

$$-w_1'' = \sigma_1w_1 + (D_1 + a(x)\psi_1)\psi_1. \quad (2.11)$$

Therefore, multiplying by  $\psi_1$  this equation and integrating in  $(0, 1)$  yields

$$D_1 = -\frac{\int_0^1 a(x)\psi_1^3(x) dx}{\int_0^1 \psi_1^2(x) dx} = -2 \int_0^1 a(x) \sin^3(\pi x) dx. \quad (2.12)$$

If  $D_1 \neq 0$ , then, since  $a(x)$  changes the sign, the *bifurcation direction*,  $D = D_1$ , can take any value, either positive, or negative. Actually, the bifurcation to positive solutions is supercritical if  $D > 0$ , while it is subcritical if  $D < 0$ . If  $D_1 = 0$ , then we need to compute  $D_2$ . Suppose  $D_1 = 0$ . Then, similarly as above, we can collect terms of the second order in  $s$  from (2.10) to get

$$-w_2'' = \sigma_1w_2 + D_2\psi_1 + a(x)w_1\psi_1$$

and hence,

$$D_2 = -\frac{\int_0^1 a(x)w_1(x)\psi_1^2(x) dx}{\int_0^1 \psi_1^2(x) dx} = -2 \int_0^1 a(x)w_1(x) \sin^2(\pi x) dx. \quad (2.13)$$

Thus, to get the exact value of  $D_2$ , we need to determine  $w_1(x)$ . It is the unique solution of (2.11), subject to Dirichlet boundary conditions, in the closed subspace  $Y$ . Since  $D_1 = 0$ , the general solution of (2.11) is given by

$$w_1(x) = \cos(\pi x) \left( c_1 + \frac{1}{\pi} \int_0^x a(s) \sin^3(\pi s) ds \right) \\ + \sin(\pi x) \left( c_2 - \frac{1}{\pi} \int_0^x a(s) \sin^2(\pi s) \cos(\pi s) ds \right).$$

As  $0 = w_1(0) = c_1$ , after some adjustment we find that

$$w_1(x) = c_2 \sin(\pi x) + \frac{1}{\pi} \int_0^x a(s) \sin^2(\pi s) \sin(\pi s - \pi x) ds.$$

To find out  $c_2$ , we recall that  $y_1(s) \in Y$  for  $s \simeq 0$ . Since  $Y$  is closed, this entails that

$$w_1 = \lim_{s \rightarrow 0} \frac{y_1(s)}{s} \in Y.$$

Thus,

$$0 = \int_0^1 w_1(x) \sin(\pi x) dx \\ = c_2 \int_0^1 \sin^2(\pi x) dx + \int_0^1 \frac{\sin(\pi x)}{\pi} \int_0^x a(s) \sin^2(\pi s) \sin(\pi s - \pi x) ds dx$$

and therefore,

$$c_2 = -2 \int_0^1 \frac{\sin(\pi x)}{\pi} \int_0^x a(s) \sin^2(\pi s) \sin(\pi s - \pi x) ds dx.$$

This way we can compute the *bifurcation direction*  $D = D_2$  when  $D_1 = 0$ . This situation arises in Sections 5, 6. Should it be  $D_2 = 0$ , then it is necessary to use higher order terms of  $\lambda_1(s)$  and  $y_1(s)$ .

Next, we will use the Schauder formula for determining the Leray–Schauder degree  $\text{Deg}(\mathfrak{L}(\lambda), B_R)$ ,  $R > 0$ , for every  $\lambda \in \mathbb{R} \setminus \Sigma(\mathfrak{L})$ , where  $B_R$  stands for the open ball of radius  $R$  centered at the origin in the real Banach space  $C_0^1[0, 1]$ . According to it, we already know that

$$\text{Deg}(\mathfrak{L}(\lambda), B_R) = (-1)^{m(\mathfrak{L}(\lambda))}, \quad (2.14)$$

where  $m(\mathfrak{L}(\lambda))$  stands for the sum of the algebraic multiplicities of the negative eigenvalues of  $\mathfrak{L}(\lambda)$ . To determine  $m(\mathfrak{L}(\lambda))$ , we will find out all the values of  $\mu \in \mathbb{R}$  for which there exists  $u \in C_0^1[0, 1]$ ,  $u \neq 0$ , such that

$$\mathfrak{L}(\lambda)u = u - \lambda \mathcal{K}u = \mu u. \quad (2.15)$$

Since  $\mathfrak{L}(\lambda)$  is invertible for all  $\lambda \in (0, \sigma_1)$ , by the homotopy invariance of the degree,

$$d_1 \equiv \text{Deg}(\mathfrak{L}(\lambda), B_R) \quad \text{is constant on } \lambda \in (0, \sigma_1).$$

Similarly, for every  $k \geq 2$ ,

$$d_{k+1} \equiv \text{Deg}(\mathfrak{L}(\lambda), B_R) \quad \text{is constant on } \lambda \in (\sigma_k, \sigma_{k+1}).$$

The equation (2.15) can be expressed as

$$\mathcal{K}u = \frac{1 - \mu}{\lambda} u,$$

or, equivalently, by inverting  $\mathcal{K}$ ,

$$-u'' = \frac{\lambda}{1-\mu}u \quad \text{in } [0, 1].$$

Note that, due to (2.15),  $\mathcal{K}u = 0$  if  $\mu = 1$ , because  $\lambda > 0$ , and hence  $u = 0$ . Thus,  $\mu \neq 1$  and hence, we can divide by  $1 - \mu$ . Consequently, there should exist some integer  $n \geq 1$  such that

$$\frac{\lambda}{1-\mu} = \sigma_n$$

for some  $n \geq 1$ . Therefore, the set of (classical) eigenvalues of  $\mathfrak{L}(\lambda)$  is given by

$$\sigma(\mathfrak{L}(\lambda)) = \left\{ \mu_n := 1 - \frac{\lambda}{\sigma_n} : n \in \mathbb{N}, n \geq 1 \right\}. \quad (2.16)$$

On the other hand, for every  $\lambda > 0$  and any integer  $n \geq 1$ , the eigenvalue  $\mu_n := 1 - \frac{\lambda}{\sigma_n}$  is an algebraically simple eigenvalue of  $\mathfrak{L}(\lambda) = I - \lambda\mathcal{K}$ , because

$$N[I - \lambda\mathcal{K} - \mu_n I] = \text{span}[\psi_n] \quad \text{and} \quad \psi_n \notin R[I - \lambda\mathcal{K} - \mu_n I]. \quad (2.17)$$

Indeed, arguing by contradiction, assume that, for some  $u \in \mathcal{C}_0^1[0, 1]$ ,

$$\psi_n = u - \lambda\mathcal{K}u - \mu_n u = (1 - \mu_n)u - \lambda\mathcal{K}u.$$

Then,

$$(1 - \mu_n)u = \lambda\mathcal{K}u + \psi_n \in \mathcal{C}_0^2[0, 1]$$

and, since  $\mu_n \neq 1$ ,  $u \in \mathcal{C}_0^2[0, 1]$ . Thus, differentiating twice with respect to  $x$  yields

$$-(1 - \mu_n)u'' = \lambda u - \psi_n'' = \lambda u + \sigma_n \psi_n.$$

Equivalently, by definition of  $\mu_n$ ,

$$-\frac{\lambda}{\sigma_n}u'' - \lambda u = \sigma_n \psi_n$$

and hence,

$$-u'' - \sigma_n u = \frac{\sigma_n^2}{\lambda} \psi_n.$$

Finally, multiplying by  $\psi_n$  and integrating in  $(0, 1)$ , we find that

$$\frac{\sigma_n^2}{\lambda} \int_0^1 \psi_n^2 = \int_0^1 [(-u'' - \sigma_n u)\psi_n] = 0,$$

which is impossible. This ends the proof of (2.17). Therefore, (2.14) becomes

$$\text{Deg}(\mathfrak{L}(\lambda), B_R) = (-1)^{n(\lambda)}, \quad (2.18)$$

where  $n(\lambda)$  stands for the number of negative eigenvalues of (2.16). Assume  $\lambda < \sigma_1$ . Then,  $\frac{\lambda}{\sigma_1} < 1$  and, since  $\sigma_n \geq \sigma_1$  for each  $n \geq 1$ , we find that

$$1 - \frac{\lambda}{\sigma_n} \geq 1 - \frac{\lambda}{\sigma_1} > 0.$$

Thus,  $n(\lambda) = 0$  and (2.18) entails  $\text{Deg}(\mathfrak{L}(\lambda), B_R) = 1$ . Assume  $\sigma_1 < \lambda < \sigma_2$ . Then,

$$1 - \frac{\lambda}{\sigma_1} < 0 < 1 - \frac{\lambda}{\sigma_2} < 1 - \frac{\lambda}{\sigma_3} < \dots$$

and hence,  $n(\lambda) = 1$ . Therefore, by (2.18),  $\text{Deg}(\mathfrak{L}(\lambda), B_R) = -1$ . Obviously, every time that  $\lambda$  crosses an additional eigenvalue  $\sigma_n$ ,  $n(\lambda)$  increases by 1. Therefore, for every integer  $k \geq 1$ ,

$$\text{Deg}(\mathfrak{L}(\lambda), B_R) = \begin{cases} 1 & \text{if } \lambda \in (\sigma_{2k}, \sigma_{2k+1}), \\ -1 & \text{if } \lambda \in (\sigma_{2k+1}, \sigma_{2k+2}). \end{cases} \quad (2.19)$$

Consequently, according to [38, Th. 6.2.1], the next result holds. We are denoting by  $\mathcal{S}$  the set of non-trivial solutions of (1.1), i.e.,

$$\mathcal{S} = \{(\lambda, u) \in \mathfrak{F}^{-1}(0) : u \neq 0\} \cup \{(\sigma_n, 0) : n \geq 1\} \subset \mathbb{R} \times \mathcal{C}_0^1[0, 1],$$

where  $\mathfrak{F}(\lambda, u)$  is the operator introduced in (2.6).

**Theorem 2.2.** *For every  $n \geq 1$ , there exists a component of  $\mathcal{S}$ ,  $\mathcal{C}_n$ , such that  $(\sigma_n, 0) \in \mathcal{C}_n$ . Moreover, for sufficiently small  $\varepsilon > 0$ ,*

$$B_\varepsilon(\sigma_n, 0) \cap \mathcal{C}_n = \{(\lambda_n(s), s(\psi_n + y_n(s))) : s \sim 0\},$$

where  $(\lambda_n(s), s(\psi_n + y_n(s)))$ ,  $s \sim 0$ , is the analytic curve given by Theorem 2.1.

As the nodes of the solutions of (1.1) are simple, it is easily seen that the number of nodes of the solutions of (1.1) vary continuously in  $\mathbb{R} \times \mathcal{C}_0^1[0, 1]$  and hence, since the solutions of  $\mathcal{C}_n$  bifurcating from  $u = 0$  at  $\lambda = \sigma_n$  possess  $n - 1$  interior nodes in  $(0, 1)$ ,  $\mathcal{C}_n \setminus \{(\sigma_n, 0)\}$  consists of solutions with  $n - 1$  interior nodes. Therefore,

$$\mathcal{C}_n \cap \mathcal{C}_m = \emptyset \quad \text{if } n \neq m.$$

Consequently, thanks to the global alternative of P. H. Rabinowitz [60],  $\mathcal{C}_n$  is unbounded in  $\mathbb{R} \times \mathcal{C}_0^1[0, 1]$  for each integer  $n \geq 1$ . Note that  $\mathcal{C}^+$  is the subcomponent of  $\mathcal{C}_1$  consisting of the positive solutions  $(\lambda, u) \in \mathcal{C}_1$ . According to [38, Th. 6.4.3],  $\mathcal{C}^+$  also is unbounded in  $\mathbb{R} \times \mathcal{C}_0^1[0, 1]$ . A further rather standard compactness argument, whose details are omitted here, shows that actually  $\mathcal{C}^+$  is unbounded in  $\mathbb{R} \times \mathcal{C}_0[0, 1]$ . This information can be summarized into the next result.

**Theorem 2.3.** *The component  $\mathcal{C}^+$  is unbounded in  $\mathbb{R} \times \mathcal{C}_0[0, 1]$ . Moreover,  $\lambda = \pi^2$  if  $(\lambda, 0) \in \mathcal{C}^+$ . Furthermore,  $\mathcal{C}^+$  bifurcates supercritically from  $u = 0$  at  $\lambda = \pi^2$  if  $D > 0$ , while it does it subcritically if  $D < 0$ , where  $D$  is given by (2.12) or (2.13).*

In addition, thanks to the a priori bounds of H. Amann and J. López-Gómez [3], the next result holds.

**Theorem 2.4.** *The component  $\mathcal{C}^+$  is uniformly bounded on any compact subinterval of  $\lambda \in \mathbb{R}$ , and (1.1) cannot admit a positive solution for sufficiently large  $\lambda$ . Thus,*

$$(-\infty, \pi^2) \subset \mathcal{P}_\lambda(\mathcal{C}^+).$$

Moreover, if (1.1) admits a positive solution,  $(\lambda_0, u_0)$ , with  $\lambda_0 > \pi^2$ , then it admits at least two positive solutions for every  $\lambda \in (\pi^2, \lambda_0)$ .

These findings can be complemented with the theory of R. Gómez-Reñasco and J. López-Gómez [28, 29], later refined in [41], up to characterize the existence of linearly stable positive solutions of (1.1) thorough the sign of  $D$ . Indeed, by [41, Cor. 9.10], any positive solution of (1.1) is linearly unstable if  $D \leq 0$ , and actually, due to [41, Pr. 9.2], (1.1) cannot admit a positive solution  $(\lambda, u)$  with  $\lambda \geq \pi^2$  in such case. Thus,

$$\mathcal{P}_\lambda(\mathcal{C}^+) = (-\infty, \pi^2)$$

if  $D \leq 0$ . Moreover, (1.1) admits some stable positive solution if, and only if,  $D > 0$  and, in such case, the results of [41, Sec. 9.2-4], provide us with the next one.

**Theorem 2.5.** *Assume  $D > 0$ . Then, there exists  $\lambda_t > \pi^2$  such that (1.1) cannot admit a positive solution if  $\lambda > \lambda_t$ , and*

$$\mathcal{P}_\lambda(\mathcal{C}^+) = (-\infty, \lambda_t].$$

Moreover,

- (a) Any positive solution of (1.1) with  $\lambda \leq \pi^2$  is linearly unstable.
- (b) For every  $\lambda \in (\pi^2, \lambda_t]$ , the minimal positive solution of (1.1),  $(\lambda, \theta_\lambda^{\min})$ , is the unique stable positive solution of (1.1). Moreover, these solutions are linearly stable if  $\lambda \in (\pi^2, \lambda_t)$ . Thus, they are local exponential attractors of (1.7).
- (c) For every  $\lambda \in (\pi^2, \lambda_t)$ , (1.1) possesses, at least, two positive solutions: one linearly stable and another one unstable.
- (d)  $(\lambda_t, \theta_{\lambda_t}^{\min})$  is the unique positive solution of (1.1) at  $\lambda = \lambda_t$ , and it is linearly neutrally stable. Moreover, the set of positive solutions of (1.1) in a neighborhood of  $(\lambda_t, \theta_{\lambda_t}^{\min})$  consists of a quadratic subcritical turning point whose lower half-curve is filled in by linearly stable positive solutions, while its upper half-curve consists of unstable solutions with one-dimensional unstable manifold.
- (e) The map  $\lambda \rightarrow \theta_\lambda^{\min}$ ,  $(\sigma_1, \lambda_t) \rightarrow \mathcal{C}_0^1[0, 1]$ , is analytic and

$$\lim_{\lambda \uparrow \lambda_t} \theta_\lambda^{\min} = \theta_{\lambda_t}^{\min}.$$

The numerical experiments carried out in this paper confirm and illuminate these findings complementing them. Note that the *exchange stability principle* of M. G. Crandall and P. H. Rabinowitz [16] only provides us with the linearized stability of the minimal positive solution for  $\lambda > \pi^2$  sufficiently close to  $\pi^2$ , while the existence and the uniqueness of the stable positive solution established by Theorem 2.5 inherits a global character. Very recently, it has been established by S. Fernández-Rincón and J. López-Gómez [26] that choosing a nonlinearity of the type  $u^p$  for some  $p \geq 2$  in (1.1) is imperative for the validity of Theorem 2.5, regardless the nature of the boundary conditions that might be of general type. This explains why in this paper we are focusing attention on the particular example (1.1).

### 3. A MULTIPLICITY RESULT AS $\lambda \downarrow -\infty$

The next result provides us with the point-wise behavior of the positive solutions of (1.1) in

$$\Omega_- := a^{-1}((-\infty, 0)) = \text{intsupp } a^-.$$

**Theorem 3.1.** *For every  $\lambda < \pi^2$ , let  $u_\lambda$  be a positive solution of (1.1). Then,*

$$\lim_{\lambda \downarrow -\infty} u_\lambda(x) = 0 \quad \text{for all } x \in \Omega_- \tag{3.1}$$

uniformly on compact subintervals of  $\Omega_-$ .

*Proof.* Pick an arbitrary  $x_0 \in \Omega_-$ . As  $\Omega_-$  is open, there exists  $\varepsilon > 0$  such that

$$0 < x_0 - 4\varepsilon < x_0 + 4\varepsilon < 1 \quad \text{and} \quad [x_0 - 4\varepsilon, x_0 + 4\varepsilon] \subset \Omega_-.$$

Since  $a$  is continuous, we have that

$$\omega := \max_{|x-x_0| \leq 4\varepsilon} a(x) < 0.$$

Let  $\ell_\lambda^{\min}$  denote the minimal positive solution of the singular problem

$$\begin{cases} -\ell'' = \lambda \ell + a(x)\ell^2 & \text{in } (x_0 - 4\varepsilon, x_0 + 4\varepsilon), \\ \ell(x_0 - 4\varepsilon) = \ell(x_0 + 4\varepsilon) = \infty, \end{cases} \tag{3.2}$$

whose existence is guaranteed by, e.g., [41, Ch. 3], and set

$$B := \|\ell_\lambda^{\min}\|_{\mathcal{C}[x_0-2\varepsilon, x_0+2\varepsilon]}.$$

Then, the restriction of the function  $\ell_\lambda^{\min}$  to the interval  $[x_0 - 2\varepsilon, x_0 + 2\varepsilon]$  provides us with a positive subsolution of the regular problem

$$\begin{cases} -u'' = \lambda u + \omega u^2 & \text{in } (x_0 - 2\varepsilon, x_0 + 2\varepsilon), \\ u(x_0 - 2\varepsilon) = u(x_0 + 2\varepsilon) = B. \end{cases} \quad (3.3)$$

As  $\omega < 0$ , any sufficiently large constant,  $M > B$ , provides us with a supersolution of (3.3) such that

$$\ell_\lambda^{\min} < M \quad \text{in } [x_0 - 2\varepsilon, x_0 + 2\varepsilon].$$

Thus, thanks to, e.g., [41, Th. 2.4], (3.3) possesses a unique positive solution,  $\theta_{[\lambda, B]}$ , such that

$$\ell_\lambda^{\min} \leq \theta_{[\lambda, B]} \leq M \quad \text{in } [x_0 - 2\varepsilon, x_0 + 2\varepsilon].$$

Moreover, according to the proof of [41, Th 3.2],  $\theta_{[\lambda, B]}$  is symmetric about  $x_0$ , and, for every  $\lambda \in \mathbb{R}$ , the point-wise limit

$$L_\lambda := \lim_{\xi \uparrow \infty} \theta_{[\lambda, \xi]}$$

is increasing and, thanks to the uniqueness result of [39], it provides us with the unique positive solution of the singular problem

$$\begin{cases} -u'' = \lambda u + \omega u^2 & \text{in } (x_0 - 2\varepsilon, x_0 + 2\varepsilon), \\ u(x_0 - 2\varepsilon) = u(x_0 + 2\varepsilon) = \infty. \end{cases}$$

Since  $L_\lambda$  is symmetric about  $x_0$ , it is apparent that

$$L_\lambda(x_0) = \min_{(x_0 - 2\varepsilon, x_0 + 2\varepsilon)} L_\lambda. \quad (3.4)$$

On the other hand, by [41, Th. 2.4], we already know that  $\theta_{[\lambda, \xi]} < \theta_{[\mu, \xi]}$  if  $\lambda < \mu$ . Thus, letting  $\xi \uparrow \infty$  yields

$$L_\lambda \leq L_\mu \quad \text{in } [x_0 - 2\varepsilon, x_0 + 2\varepsilon].$$

Subsequently, we consider the auxiliary function

$$\varphi(x) := \sin \frac{\pi(x - x_0 + \varepsilon)}{2\varepsilon}, \quad x \in [x_0 - \varepsilon, x_0 + \varepsilon].$$

It has been chosen to satisfy

$$\begin{cases} -\varphi'' = \left(\frac{\pi}{2\varepsilon}\right)^2 \varphi & \text{in } (x_0 - \varepsilon, x_0 + \varepsilon), \\ \varphi(x_0 - \varepsilon) = \varphi(x_0 + \varepsilon) = 0. \end{cases} \quad (3.5)$$

Thus, multiplying the differential equation

$$-L_\lambda'' = \lambda L_\lambda + \omega L_\lambda^2 \quad \text{in } [x_0 - \varepsilon, x_0 + \varepsilon]$$

by  $\varphi$  and integrating in  $(x_0 - \varepsilon, x_0 + \varepsilon)$  yields

$$-\int_{x_0 - \varepsilon}^{x_0 + \varepsilon} L_\lambda'' \varphi \, dx = \lambda \int_{x_0 - \varepsilon}^{x_0 + \varepsilon} L_\lambda \varphi \, dx + \omega \int_{x_0 - \varepsilon}^{x_0 + \varepsilon} L_\lambda^2 \varphi \, dx. \quad (3.6)$$

On the other hand, integrating by parts, we find that

$$\begin{aligned} \int_{x_0 - \varepsilon}^{x_0 + \varepsilon} L_\lambda'' \varphi \, dx &= \int_{x_0 - \varepsilon}^{x_0 + \varepsilon} (L_\lambda' \varphi)' \, dx - \int_{x_0 - \varepsilon}^{x_0 + \varepsilon} L_\lambda' \varphi' \, dx = - \int_{x_0 - \varepsilon}^{x_0 + \varepsilon} L_\lambda' \varphi' \, dx, \\ \int_{x_0 - \varepsilon}^{x_0 + \varepsilon} L_\lambda \varphi'' \, dx &= \int_{x_0 - \varepsilon}^{x_0 + \varepsilon} (L_\lambda \varphi')' \, dx - \int_{x_0 - \varepsilon}^{x_0 + \varepsilon} L_\lambda' \varphi' \, dx. \end{aligned}$$

Consequently, by (3.5),

$$\begin{aligned} - \int_{x_0-\varepsilon}^{x_0+\varepsilon} L_\lambda'' \varphi \, dx &= \int_{x_0-\varepsilon}^{x_0+\varepsilon} L_\lambda' \varphi' \, dx = \int_{x_0-\varepsilon}^{x_0+\varepsilon} (L_\lambda \varphi')' \, dx - \int_{x_0-\varepsilon}^{x_0+\varepsilon} L_\lambda \varphi'' \, dx \\ &= L_\lambda(x_0 + \varepsilon) \varphi'(x_0 + \varepsilon) - L_\lambda(x_0 - \varepsilon) \varphi'(x_0 - \varepsilon) + \left(\frac{\pi}{2\varepsilon}\right)^2 \int_{x_0-\varepsilon}^{x_0+\varepsilon} L_\lambda \varphi \, dx. \end{aligned}$$

Thus, since  $\omega < 0$ , substituting in (3.6) yields

$$\begin{aligned} \left[ \left(\frac{\pi}{2\varepsilon}\right)^2 - \lambda \right] \int_{x_0-\varepsilon}^{x_0+\varepsilon} L_\lambda \varphi \, dx &= \omega \int_{x_0-\varepsilon}^{x_0+\varepsilon} L_\lambda^2 \varphi \, dx + L_\lambda(x_0 - \varepsilon) \varphi'(x_0 - \varepsilon) - L_\lambda(x_0 + \varepsilon) \varphi'(x_0 + \varepsilon) \\ &< L_\lambda(x_0 - \varepsilon) \varphi'(x_0 - \varepsilon) - L_\lambda(x_0 + \varepsilon) \varphi'(x_0 + \varepsilon). \end{aligned}$$

Therefore, since

$$L_\lambda(x_0 - \varepsilon) \varphi'(x_0 - \varepsilon) - L_\lambda(x_0 + \varepsilon) \varphi'(x_0 + \varepsilon) > 0,$$

we can infer from the previous estimate that

$$\lim_{\lambda \downarrow -\infty} \int_{x_0-\varepsilon}^{x_0+\varepsilon} L_\lambda \varphi \, dx = 0. \quad (3.7)$$

Consequently, owing to (3.4) and (3.7), it becomes apparent that

$$\lim_{\lambda \downarrow -\infty} L_\lambda(x_0) = 0. \quad (3.8)$$

Note that, since

$$\ell_\lambda^{\min} \leq \theta_{[\lambda, B]} \leq L_\lambda \quad \text{in } (x_0 - 2\varepsilon, x_0 + 2\varepsilon),$$

(3.8) implies that

$$\lim_{\lambda \downarrow -\infty} \ell_\lambda^{\min}(x_0) = 0. \quad (3.9)$$

Similarly, for every  $x \in [x_0 - \varepsilon, x_0 + \varepsilon]$ , we have that

$$[x - \varepsilon, x + \varepsilon] \subset [x_0 - 2\varepsilon, x_0 + 2\varepsilon]$$

and hence, the restriction of  $\ell_\lambda^{\min}$  to the interval  $[x - \varepsilon, x + \varepsilon]$  provides us with a subsolution of

$$\begin{cases} -u'' = \lambda u + \omega u^2 & \text{in } (x - \varepsilon, x + \varepsilon), \\ u(x - \varepsilon) = u(x + \varepsilon) = B. \end{cases} \quad (3.10)$$

Consequently, reasoning as above, it becomes apparent that

$$\ell_\lambda^{\min} \leq L_{\lambda, x} \quad \text{in } (x - \varepsilon, x + \varepsilon), \quad (3.11)$$

where  $L_{\lambda, x}$  stands for the unique positive solution of the singular problem

$$\begin{cases} -u'' = \lambda u + \omega u^2 & \text{in } (x - \varepsilon, x + \varepsilon), \\ u(x - \varepsilon) = u(x + \varepsilon) = \infty. \end{cases}$$

By the uniqueness and the radial symmetry of  $L_{\lambda, x}$  about  $x$ , we find that

$$L_{\lambda, x}(y) = L_\lambda(x_0 - x + y) \quad \text{for all } y \in (x - \varepsilon, x + \varepsilon).$$

Thus, it follows from (3.11) that

$$\ell_\lambda^{\min}(x) \leq L_{\lambda, x}(x) = L_\lambda(x_0) \quad \text{for all } x \in (x_0 - \varepsilon, x_0 + \varepsilon).$$

Therefore, due to (3.8), we find that

$$\lim_{\lambda \downarrow -\infty} \ell_\lambda^{\min} = 0 \quad \text{uniformly in } (x_0 - \varepsilon, x_0 + \varepsilon).$$

A compactness argument ends the proof.  $\square$

As already discussed in Section 1, thanks to Theorem 3.1, the next conjecture, going back to [28], should be true. It is strongly supported by all our numerical experiments in the next sections.

**Conjecture 3.1.** *Suppose that  $a(x)$  possesses  $n + 1$  intervals where it is positive separated away by  $n$  intervals where it is negative. Then, there exists  $\lambda_c < \pi^2$  such that, for every  $\lambda < \lambda_c$ , the problem (1.1) admits, at least,  $2^{n+1} - 1$  positive solutions.*

Now, we are going to give an heuristic proof of this conjecture for the special case when  $a(x)$  is given by either (1.2), with  $n \geq 1$ , or (1.3). Actually, the proof is valid for any function  $a(x)$  symmetric about 0.5 and consisting of sinusoidal functions on each of the components of  $\text{supp } a^+$ , say  $I_j^+$ ,  $1 \leq j \leq n + 1$ . Our proof is rigorous, except for a technical detail that has been confirmed numerically. With the notations of Section 1, suppose that

$$I_j^+ = [\alpha_j, \beta_j], \quad j \in \{1, \dots, n + 1\},$$

and, for every  $j \in \{1, \dots, n + 1\}$  and  $\lambda < \left(\frac{\pi}{\beta_j - \alpha_j}\right)^2$ , let us denote by  $\theta_{\{\lambda, j\}}$  the unique positive solution of (1.6) on  $\mathcal{C}^+$ . The existence follows from the a priori bounds of [3]. The uniqueness might be an open problem even for the special case when

$$a|_{I_j^+}(x) = \mu_j \sin \frac{\pi(x - \alpha_j)}{\beta_j - \alpha_j}, \quad x \in [\alpha_j, \beta_j], \quad (3.12)$$

for some  $\mu_j > 0$ . As, for every  $\lambda < 0$ , the change of variable  $u \equiv -\lambda U$  transforms (1.6) into

$$\begin{cases} -\varepsilon U'' = -U + a^+(x)U^2 & \text{in } (\alpha_j, \beta_j), \\ U(\alpha_j) = U(\beta_j) = 0, \end{cases} \quad (3.13)$$

with  $\varepsilon = -1/\lambda$ , it turns out that the problem of the uniqueness of the positive solution of (3.12) as  $\lambda \downarrow -\infty$  is equivalent to the problem of the uniqueness of the positive solution for the singular perturbation problem (3.13) as  $\varepsilon \downarrow 0$ . Although there is a huge amount of literature on multi-peak solutions for Schrödinger type equations like (3.13) (see, e.g., A. Ambrosetti, M. Badiale and S. Cingolani [4], M. del Pino and P. Felmer [19, 20], E. N. Dancer and J. Wei [18], and J. Wei [63]), rather astonishingly, the experts in this field still seem to be focusing most of their efforts into the problem of the existence of multi-bump solutions, rather than on the problem of their uniqueness (see, e.g., the recent paper of Y. Le, J. Wei and H. Xu [35]).

Nevertheless, our numerical experiments suggest that the problem (1.6), for the special choice (3.12), possesses a unique positive solution,  $\theta_{\lambda, j}$ , on  $\mathcal{C}^+$  for every  $\lambda < \pi^2$ . Moreover,  $\theta_{\lambda, j}$  is symmetric about the central point of  $(\alpha_j, \beta_j)$ ,  $z_j := \frac{\alpha_j + \beta_j}{2}$ , where the function  $a|_{I_j^+}$  reaches its maximum value in  $I_j^+$ , and it has a single peak at  $z_j$ . Naturally, since  $a|_{I_j^+}$  is symmetric about  $z_j$ , the problem (1.6) admits a symmetric positive solution, which can be constructed by merging the two positive solutions of the boundary value problems

$$\begin{cases} -u'' = \lambda u + a^+(x)u^2 & \text{in } (\alpha_j, z_j), \\ u(\alpha_j) = 0, \quad u'(z_j) = 0, \end{cases} \quad \begin{cases} -u'' = \lambda u + a^+(x)u^2 & \text{in } (z_j, \beta_j), \\ u'(z_j) = 0, \quad u(\beta_j) = 0. \end{cases} \quad (3.14)$$

Our numerical experiments suggest that

$$\mathcal{C}^+ = \left\{ (\lambda, \theta_{\lambda, j}) : \lambda < \left(\frac{\pi}{\beta_j - \alpha_j}\right)^2 \right\}$$

consists of symmetric solutions about  $z_j$ , because we could not find any secondary bifurcation point along the curve  $\mathcal{C}^+$ . Figure 1 shows the global bifurcation diagram of positive solutions of (1.6) for the special choice (3.12), with  $\mu_j = 1$ , after re-scaling the problem to the entire

interval  $[0, 1]$ . We are plotting the parameter  $\lambda$ , in abscisas, versus the derivative of the solution at the origin,  $u'(0)$ , in ordinates. As for  $\lambda < -600$ ,  $\theta'_{\lambda,j}(0)$  is very small, for this range of values of  $\lambda$  it is hard to differentiate  $\mathcal{C}^+$  from the  $\lambda$ -axis. The component  $\mathcal{C}^+$  bifurcates subcritically from  $u = 0$  at  $\lambda = \pi^2$  and, according to [3], satisfies  $\mathcal{P}_\lambda(\mathcal{C}^+) = (-\infty, \pi^2)$ . It consists of symmetric solutions about 0.5 with a single peak at 0.5.

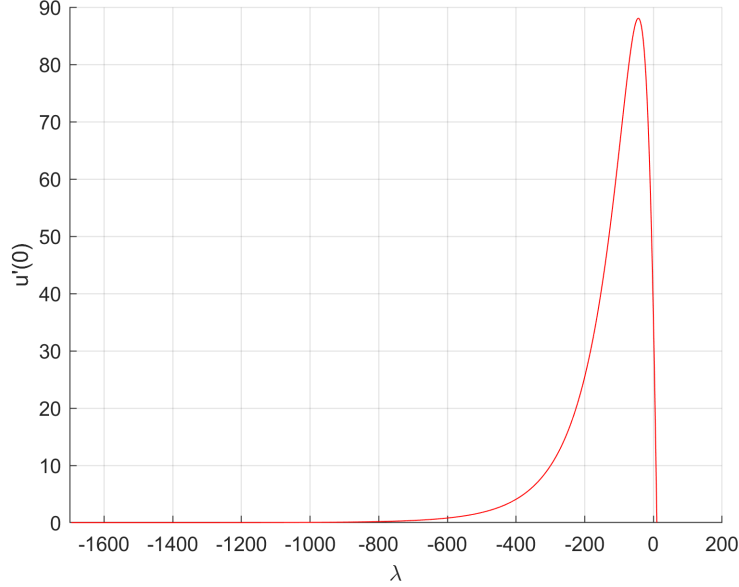


FIGURE 1. Global bifurcation diagram of (1.6).

Figure 2 shows the plots of the solutions of  $\mathcal{C}^+$  corresponding to  $\lambda = -100$ ,  $\lambda = -683$  and  $\lambda = -1695$ , respectively. Not surprisingly, the smaller is the value of  $\lambda$ , the more concentrated is the mass of  $\theta_{\lambda,j}$  at 0.5. It should not be forgotten that the three solutions plotted in Figure 2 have been previously re-scaled to the interval  $[0, 1]$  from the original interval  $[\alpha_j, \beta_j]$  in such a way that 0.5 corresponds to  $z_j$ . Actually, according to our numerical experiments, it becomes apparent that, for every  $x \in [\alpha_j, \beta_j]$ ,

$$\lim_{\lambda \downarrow -\infty} \theta_{\lambda,j}(x) = \begin{cases} +\infty & \text{if } x = z_j, \\ 0 & \text{if } x \neq z_j, \end{cases}$$

which is a genuine behavior for this type of semilinear elliptic boundary value problems of superlinear type.

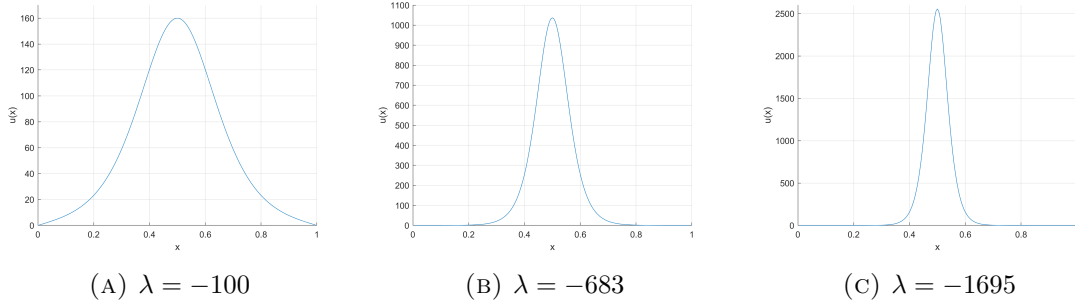
Subsequently, we will consider the subsolution of (1.1) defined by

$$\underbrace{u}_{n+1} := \begin{cases} \theta_{\lambda,j} & \text{in } [\alpha_j, \beta_j], \quad j \in \{1, \dots, n+1\}, \\ 0 & \text{in } [0, 1] \setminus \bigcup_{j=1}^{n+1} [\alpha_j, \beta_j]. \end{cases} \quad (3.15)$$

The fact that this function provides us with a weak subsolution of (1.1) is a direct consequence of a result of H. Berestycki and P. L. Lions [7]. Thus, making the choice

$$u_0 := \underline{u}_{1\dots 1},$$

by the theory of D. Sattinger [61], it becomes apparent that the unique solution of the associated parabolic problem (1.7), denoted by  $u(x, t; u_0)$  for all time  $t \in I_{\max} := [0, T_{\max}(u_0))$ ,


 FIGURE 2. Three positive solutions of the component  $\mathcal{C}^+$ .

where  $T_{\max}(u_0) \in (0, +\infty)$  stands for the maximal existence time of  $u(x, t; u_0)$ , must be a subsolution of (1.1) for all  $t \in I_{\max}$ . Equivalently,  $u(x, t; u_0)$  is non-decreasing for all  $t \in I_{\max}$ . In particular,

$$u_0 \leq u(\cdot, t; u_0) \text{ in } [0, 1] \text{ for all } t \in I_{\max}. \quad (3.16)$$

Moreover, by the main theorem of H. Matano [57], for every  $t \in I_{\max}$ , the solution  $u(\cdot, t; u_0)$  cannot admit more than  $n + 1$  peaks in  $(0, 1)$ , and, since  $u_0$  is symmetric about 0.5, as well as  $a(x)$ , it becomes apparent that  $u(\cdot, t; u_0)$  must be also symmetric for all  $t \in I_{\max}$ .

Now, observe that, on each compact subinterval of  $[0, 1]$  where  $a \leq 0$ , say  $I^-$ ,

$$\frac{\partial u}{\partial t} = \frac{\partial^2 u}{\partial x^2} + \lambda u + a u^2 \leq \frac{\partial^2 u}{\partial x^2},$$

because  $u > 0$  and  $\lambda < 0$ . Thus, by the weak maximum principle, for every  $T \in I_{\max}$ ,

$$\max_{x \in \partial_L Q_T} u(x, T; u_0) = \max_{x \in Q_T} u(x, T; u_0),$$

where  $Q_T$  stands for the parabolic cylinder  $Q_T = I^- \times [0, T]$  and  $\partial_L Q_T$  stands for the lateral boundary of  $Q_T$ :

$$\partial_L Q_T = (I^- \times \{0\}) \cup (\partial I^- \times [0, T]).$$

Actually, by the strong maximum principle of L. Nirenberg [58],  $u(x, t; u_0)$  cannot take its maximum in the interior of  $Q_T$ , at some point  $(x_M, t_M)$ , unless  $u$  is constant for all  $t \in [0, t_M]$ , which is impossible, because  $u(x, 0; u_0) = 0$  on  $I^-$  and  $u(x, t; u_0) > 0$  for all  $x \in (0, 1)$  and  $t \in I_{\max}$ . Therefore,  $u$  cannot admit any peak on any of the components of  $\text{supp } a^-$ . As a byproduct, the peaks cannot travel, as time increases, from any component  $I_j^+$  to some other  $I_i^+$  with  $i \neq j$ . Therefore, according to the theorem of H. Matano [57], for every  $j \in \{1, \dots, n + 1\}$ , either the initial peak of  $u_0$  in  $I_j^+$  persists and it is unique for all  $t \in I_{\max}$ , or it eventually disappears at some  $t^* \in I_{\max}$ . Moreover, if it persists, at, say,  $(x_t, t)$ , then, by uniqueness,

$$\frac{\partial u}{\partial x}(x, t) \geq 0 \text{ for all } x \in [\alpha_j, x_t]. \quad (3.17)$$

We claim that there exists a constant,  $C > 0$ , such that

$$u(x, t; u_0) \leq C \text{ for all } (x, t) \in [0, 1] \times I_{\max}. \quad (3.18)$$

This, in particular, entails  $T_{\max}(u_0) = +\infty$ , i.e.,  $I_{\max} = [0, \infty)$ . Moreover, thanks to, e.g., the main theorem of M. Langlais and D. Phillips [34], the point-wise limit

$$\theta_{\{\lambda, (1, \dots, 1)\}} := \lim_{t \uparrow \infty} u(\cdot, t; u_0)$$

provides us with a positive solution of (1.1) such that  $u_0 \leq \theta_{\{\lambda, (1, \dots, 1)\}}$ . Therefore, thanks to (3.15) and Theorem 3.1, for sufficiently negative  $\lambda < 0$ , the positive solution  $\theta_{\{\lambda, (1, \dots, 1)\}}$  must have, exactly,  $n + 1$  peaks in  $[0, 1]$ , one on each of the  $n + 1$  intervals  $(\alpha_j, \beta_j)$ ,  $j \in \{1, \dots, n + 1\}$ .

To prove (3.18) we can argue by contradiction. Suppose that there is a sequence

$$(x_n, t_n) \in (0, 1) \times I_{\max}, \quad n \geq 1,$$

such that

$$u_n^* \equiv u(x_n, t_n; u_0) = \|u(\cdot, t_n; u_0)\|_\infty \rightarrow \infty \text{ as } n \rightarrow \infty. \quad (3.19)$$

Then, infinitely many of these  $x_n$ 's must lie in some of the intervals  $(\alpha_j, \beta_j)$ 's. Without loss of generality, we can assume that there exists  $j_0 \in \{1, \dots, n + 1\}$  such that  $x_n \in (\alpha_{j_0}, \beta_{j_0})$  for all  $n \geq 1$ . By (3.17), for every  $n \geq 1$ , we have that

$$\frac{\partial u}{\partial x}(x, t_n) \geq 0 \quad \text{for all } x \in [\alpha_{j_0}, x_n]. \quad (3.20)$$

Thus, at  $t = t_n$ , we find that, in  $[\alpha_{j_0}, x_n]$ ,

$$0 \leq \frac{\partial u}{\partial t} \frac{\partial u}{\partial x} \leq \frac{\partial^2 u}{\partial x^2} \frac{\partial u}{\partial x} + \lambda u \frac{\partial u}{\partial x} + a u^2 \frac{\partial u}{\partial x} \leq \frac{\partial^2 u}{\partial x^2} \frac{\partial u}{\partial x} + \lambda u \frac{\partial u}{\partial x} + \|a\|_\infty u^2 \frac{\partial u}{\partial x}$$

and hence,

$$\frac{\partial}{\partial x} \left( \frac{v^2}{2} + \frac{\lambda}{2} u^2 + \frac{\|a\|_\infty}{3} u^3 \right) \geq 0$$

in  $[\alpha_{j_0}, x_n]$  for all  $n \geq 1$ , where we are denoting  $v \equiv \frac{\partial u}{\partial x}$ . Consequently, integrating these inequalities in  $[x, x_n]$ ,  $x \in [\alpha_{j_0}, x_n]$ , it becomes apparent that, for every  $n \geq 1$  and  $x \in [\alpha_{j_0}, x_n]$ ,

$$v^2(x, t_n; u_0) \geq \lambda \left[ (u_n^*)^2 - u^2(x, t_n; u_0) \right] + \frac{2\|a\|_\infty}{3} \left[ (u_n^*)^3 - u^3(x, t_n; u_0) \right].$$

So, taking into account (3.20), we find that

$$\begin{aligned} x_n - \alpha_{j_0} &= \int_{\alpha_{j_0}}^{x_n} \frac{\frac{\partial u}{\partial x}(x, t_n; u_0)}{v(x, t_n; u_0)} dx \\ &\leq \int_{\alpha_{j_0}}^{x_n} \frac{\frac{\partial u}{\partial x}(x, t_n; u_0)}{\sqrt{\lambda \left[ (u_n^*)^2 - u^2(x, t_n; u_0) \right] + \frac{2\|a\|_\infty}{3} \left[ (u_n^*)^3 - u^3(x, t_n; u_0) \right]}} dx \\ &= \int_{u(\alpha_{j_0}, t_n; u_0)}^{u(x_n, t_n; u_0)} \frac{d\xi}{\sqrt{\lambda \left[ (u_n^*)^2 - \xi^2 \right] + \frac{2\|a\|_\infty}{3} \left[ (u_n^*)^3 - \xi^3 \right]}} \\ &= \int_0^{u_n^*} \frac{d\xi}{\sqrt{\lambda \left[ (u_n^*)^2 - \xi^2 \right] + \frac{2\|a\|_\infty}{3} \left[ (u_n^*)^3 - \xi^3 \right]}}. \end{aligned}$$

Thus, implementing the change of variable  $\xi = u_n^* \tau$  yields to

$$x_n - \alpha_{j_0} \leq \int_0^1 \frac{d\tau}{\sqrt{\lambda(1 - \tau^2) + \frac{2u_n^*\|a\|_\infty}{3}(1 - \tau^3)}} \quad (3.21)$$

and therefore, letting  $n \rightarrow \infty$  in (3.21), we can infer from (3.19) that

$$\lim_{n \rightarrow \infty} x_n = \alpha_{j_0}.$$

In other words, under (3.19), the peak moves away towards the left end of the interval  $I_{j_0}^+$  as  $t \uparrow T_{\max}(u_0)$ . This is impossible, because it contradicts the symmetry of the solution  $u$

about 0.5. Consequently, the a priori bounds (3.18) are indeed satisfied, and the existence of a solution of (1.1) with  $n + 1$  peaks holds for sufficiently negative  $\lambda < 0$ .

Lastly, for every  $(d_1, \dots, d_{n+1}) \in \{0, 1\}^{n+1}$  with  $\sum_{i=1}^{n+1} d_i \leq n$ , we consider the initial data

$$\tilde{u}_0 := \underline{u}_{(d_1, \dots, d_{n+1})} \equiv \begin{cases} d_j \theta_{\{\lambda, j\}} & \text{in } I_j^+, & j \in \{1, \dots, n+1\}, \\ 0 & \text{in } I_i^-, & i \in \{1, \dots, n\}, \end{cases}$$

with type  $T \equiv (d_1, d_2, \dots, d_{n+1})$ . In particular, it possesses

$$|T| \equiv \sum_{i=1}^{n+1} d_i$$

peaks. Arguing as before, it is apparent that  $u(x, t; \tilde{u}_0)$  is a subsolution of (1.1) for all  $t \in I_{\max}(\tilde{u}_0)$ . Moreover, by the parabolic maximum principle, since  $\tilde{u}_0 \leq u_0$ , we have that, for every  $x \in [0, 1]$  and  $t > 0$ ,

$$u(x, t; \tilde{u}_0) \leq u(x, t; u_0).$$

Therefore, according to Theorem 3.1,

$$\theta_{\{\lambda, (d_1, \dots, d_{n+1})\}} \equiv \lim_{t \uparrow \infty} u(\cdot, t; \tilde{u}_0) \leq \lim_{t \uparrow \infty} u(\cdot, t; u_0) \equiv \theta_{\{\lambda, (1, \dots, 1)\}}$$

provides us with a positive solution of (1.1) with  $|T|$  peaks for sufficiently small  $\lambda < 0$ . Taking all possible combinations ends the proof of Conjecture 3.1. This proof is rigorous except for the feature that  $\theta_{\lambda, j}$  has a single peak in  $(\alpha_j, \beta_j)$ , which has been shown numerically.

Nevertheless, this proof is rigorous when  $a^+$  is piecewise constant on the support of  $a^+$  and symmetric about 0.5. Indeed, in this case,  $a = a_j$  in  $I_j^+$  for some positive constant  $a_j$  and hence  $\theta_{\lambda, j}$  is the unique positive solution of

$$\begin{cases} -u'' = \lambda u + a_j u^2 & \text{in } (\alpha_j, \beta_j), \\ u(\alpha_j) = u(\beta_j) = 0. \end{cases} \quad (3.22)$$

As the differential equation is autonomous, the system is conservative. Indeed, multiplying the differential equation by  $u'$  and integrating in  $[\alpha_j, x]$  yields

$$\frac{v^2(x)}{2} + \frac{\lambda}{2} u^2(x) + \frac{a_j}{3} u^3(x) = \frac{\lambda}{2} \|u\|_\infty^2 + \frac{a_j}{3} \|u\|_\infty^3 = \frac{v^2(\alpha_j)}{2} = \frac{v^2(\beta_j)}{2}$$

for all  $j \in \{1, \dots, n+1\}$  and  $x \in (\alpha_j, \beta_j)$ , where we are denoting  $v \equiv u'$ . Thus, the associated potential energy is given by

$$\varphi(\xi) = \frac{\lambda}{2} \xi^2 + \frac{a_j}{3} \xi^3.$$

Since  $\lambda < 0$ ,  $\varphi(\xi)$  is a cubic polynomial with a local maximum at  $\xi = 0$  and a local minimum at  $\xi = -\lambda/a_j > 0$ . Thus, the equilibrium  $u = 0$  is a saddle point, while  $u = -\lambda/a_j$  is a center. Therefore, by the symmetry of the system, the positive solutions reach their maximum values at  $x = 0.5$ . Moreover, since

$$0.5 = \int_0^1 \frac{d\tau}{\sqrt{\lambda(1-\tau^2) + \frac{2\|u\|_\infty a_j}{3}(1-\tau^3)}}, \quad (3.23)$$

the positive solution is unique, by the monotonicity of the integral on the right hand side of (3.23) on  $\|u\|_\infty$ . Therefore, the next result holds.

**Theorem 3.2.** *Suppose that  $a^+$  is piecewise constant and symmetric about 0.5, and its support consists of  $n + 1$  intervals separated away by  $n$  intervals where  $a < 0$ . Then, there exists  $\lambda_c < 0$  such that, for every  $\lambda < \lambda_c$ , (1.1) has, at least,  $2^{n+1} - 1$  positive solutions.*

We conjecture that, in all these cases, for sufficiently small  $\lambda < 0$ , (1.1) has, exactly,  $2^{n+1} - 1$  positive solutions.

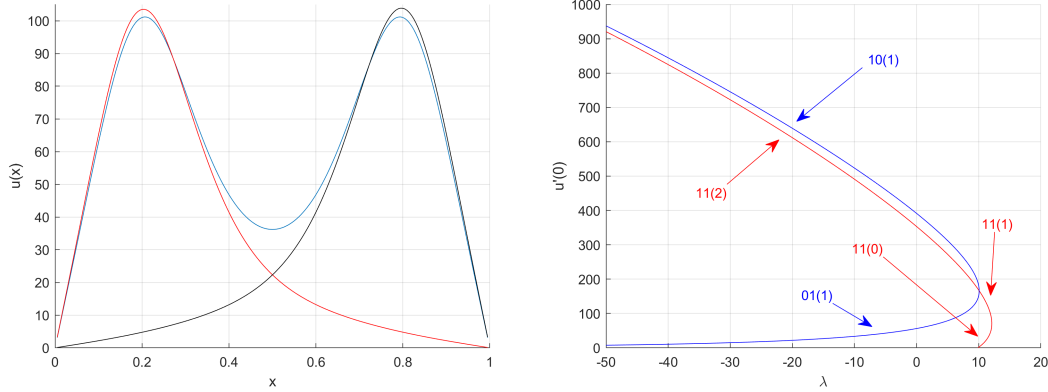
#### 4. THE CASE $n = 1$

Throughout this section, we assume that

$$a(x) = \sin(3\pi x), \quad x \in [0, 1].$$

Then, the global bifurcation diagram of the positive solutions of (1.1) looks like shows Figure 3b. Our numerical experiments suggest that the set of positive solutions of (1.1) consists of the component  $\mathcal{C}^+$ , which bifurcates supercritically from  $u = 0$  at  $\lambda = \pi^2$ , because

$$D_1 = -2 \int_0^1 a(x) \sin^3(\pi x) dx = -2 \int_0^1 \sin(3\pi x) \sin^3(\pi x) dx = \frac{1}{4} > 0.$$



(A) Positive solutions for  $\lambda \approx -21$ : 10(1) in red, 01(1) in black, and 11(2) in blue.

(B) Global bifurcation diagram.

FIGURE 3. Numerical results for  $a(x) = \sin(3\pi x)$ .

This component exhibits a turning point at  $\lambda_t \approx 12.1$ , and a secondary bifurcation at  $\lambda_s \approx 10.1$ , as shown in the global bifurcation diagram plotted in Figure 3b. In this and in all subsequent global bifurcation diagrams we are plotting the parameter  $\lambda$ , in abscissas, versus the derivative of the solution at the origin,  $u'(0)$ , in ordinates. This allows to differentiate between all admissible positive solutions. By the symmetries of the problem, the reflection about 0.5 of any positive solution of (1.1) provides with another solution, though there is no way to differentiate between such solutions if, instead of plotting  $\lambda$  versus  $u'(0)$ , we plot  $\lambda$  versus the  $L_p$ -norm of the solutions for some  $p \geq 1$ . Should we proceed in this way, we could not differentiate between, e.g., the solutions of types 01(1) and 10(1), as they have the same  $L_p$ -norms for all  $p \geq 1$  (see the plots of these solutions in Figure 3a).

According to Theorem 2.5,  $\mathcal{P}_\lambda(\mathcal{C}^+) = (-\infty, \lambda_t]$  and, for every  $\lambda \in (\pi^2, \lambda_t]$ , the minimal positive solution of (1.1) is the unique stable positive solution of (1.1). Actually, for every  $\lambda \in (\pi^2, \lambda_t)$ , the minimal solution is linearly asymptotically stable and hence, its Morse index equals zero. Moreover, by Theorem 2.5,  $(\lambda_t, \theta_{\lambda_t}^{\min})$  is the unique positive solution at  $\lambda_t$ , it is linearly neutrally stable, and it is a quadratic subcritical turning point of the component  $\mathcal{C}^+$ . The solutions on the upper half curve through the subcritical turning point  $(\lambda_t, \theta_{\lambda_t}^{\min})$  have one-dimensional unstable manifold, and actually are of type 11(1) until  $\lambda$  reaches the

secondary bifurcation point,  $\lambda_s$ , where they became unstable with Morse index two and type 11(2) for any further smaller value of  $\lambda$ .

At  $\lambda = \lambda_s$ , two (new) secondary branches of positive solutions with respective types 01(1) and 10(1) bifurcate subcritically. Naturally,  $u'(0) \approx 0$  for the solutions of type 01(1), while  $u'(0)$  is large for those of type 10(1), as confirmed by our numerical experiments. These three branches seem to be globally defined for all further smaller values of  $\lambda$ ,  $\lambda < \lambda_s$ .

In full agreement with Conjecture 3.1, the problem (1.1) has three positive solutions for every  $\lambda < \lambda_s$ . Figure 3a shows the plots of these solutions at a value  $\lambda \approx -21$ . Note that the number of peaks of the solutions coincides with the dimension of their respective unstable manifolds for all  $\lambda < \lambda_s$ .

### 5. THE CASE $n = 2$

Throughout this section we have chosen

$$a(x) = \sin(5\pi x), \quad x \in [0, 1].$$

By Conjecture 3.1, we expect to have  $2^3 - 1 = 7$  positive solution for sufficiently negative  $\lambda$ . The global bifurcation diagram computed in this case has been plotted in Figure 4.

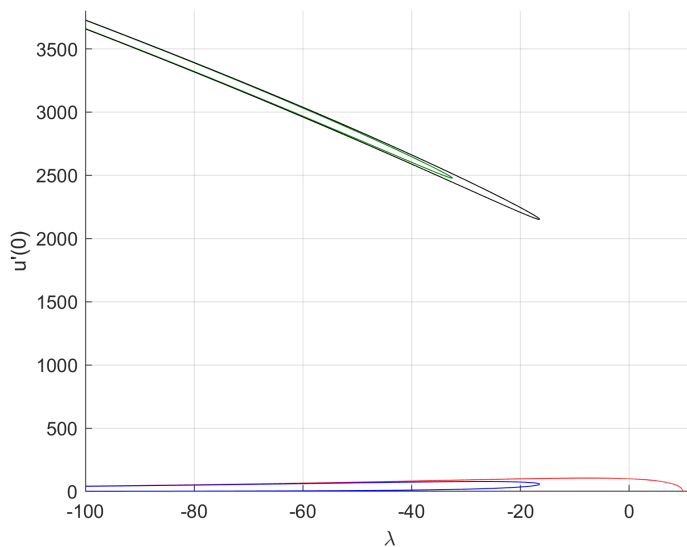


FIGURE 4. Global bifurcation diagram for  $a(x) = \sin(5\pi x)$ .

It consists of 4 components, 3 global folds isolated from  $u = 0$ , plus  $\mathcal{C}^+$ , which in this occasion bifurcates subcritically from  $u = 0$  at  $\lambda = \pi^2$ , because

$$D_1 = 2 \int_0^1 \sin(5\pi x) \sin^3(\pi x) dx = 0$$

and

$$D_2 = -2 \int_0^1 w_1(x) \sin(5\pi x) \sin^2(\pi x) dx = -\frac{5}{256\pi^2} < 0.$$

None of these components, neither  $\mathcal{C}^+$  nor any of the three folds plotted in Figure 4, exhibited any secondary bifurcation along it.

Figure 5 shows two magnifications of the most significant pieces of the global bifurcation diagram plotted in Figure 4 together with the superimposed types of the solutions along each

of the solution curves plotted on it. Precisely, Figure 5a shows a zoom of the two superior global folds plotted in Figure 4 around their respective turning points. These solutions look larger in these global bifurcation diagram because

$$\lim_{\lambda \downarrow -\infty} u'_\lambda(0) = +\infty$$

for any positive solution  $(\lambda, u_\lambda)$  having mass in  $(0, 0.2)$ . Figure 5a shows the types of the positive solutions along each of the half-branches of the two folds. They change from type 100(1) to type 110(2) as they cross the turning point of the exterior component, while they are changing from type 101(2) to type 111(3) as the turning point of the interior folding is crossed.

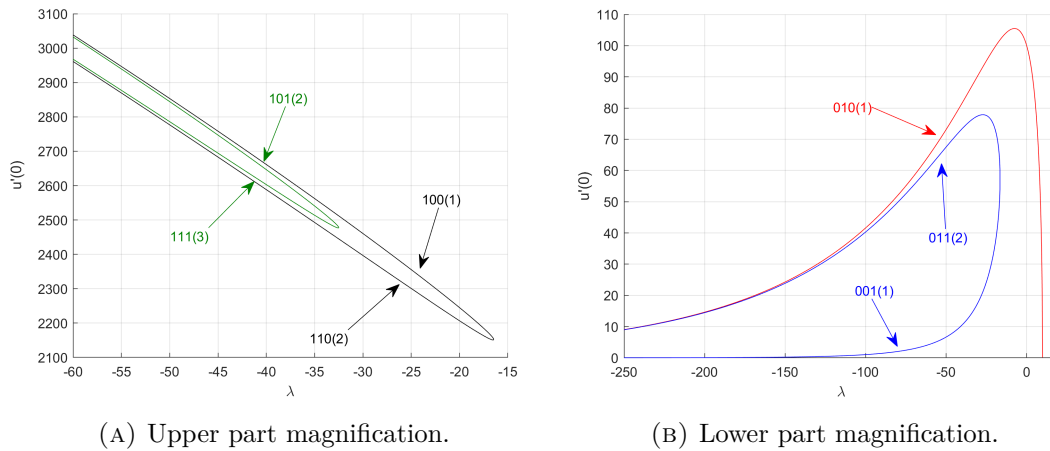


FIGURE 5. Two significant magnifications of Figure 4.

Not surprisingly, since  $\mathcal{C}^+$  does not exhibit any secondary bifurcation along it, all the solutions of  $\mathcal{C}^+$  that we have computed are of type 010(1), in complete agreement with the exchange stability principle of M. G. Crandall and P. H. Rabinowitz [16], because  $u = 0$  is linearly stable for all  $\lambda < \pi^2$ .

Lastly, the solutions along the interior folding in Figure 5b change type from 001(1) to 011(2) when the turning point of this components is switched on. Moreover, for sufficiently negative  $\lambda$ , (1.1) admits 7 positive solutions, with respective types

$$001(1), \quad 010(1), \quad 100(1), \quad 101(2), \quad 110(2), \quad 011(2), \quad 111(3),$$

in full agreement with Conjecture 3.1. In particular, in any circumstances, the number of peaks of these solutions, when they exist, equals their respective Morse indices.

## 6. THE CASE $n = 3$

Throughout this section we make the choice

$$a(x) = \sin(7\pi x), \quad x \in [0, 1].$$

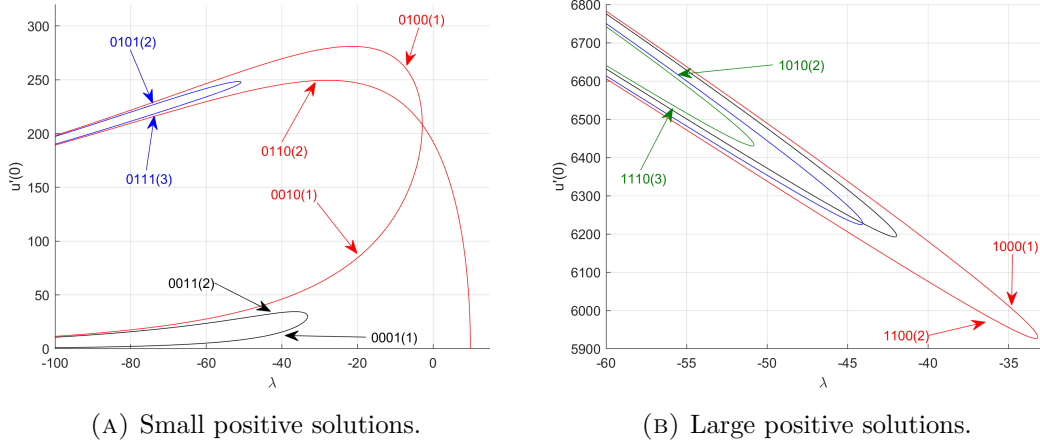
According to Conjecture 3.1, we expect to have  $2^4 - 1 = 15$  positive solution for sufficiently negative  $\lambda$ . Since

$$D_1 = -2 \int_0^1 \sin(7\pi x) \sin^3(\pi x) dx = 0$$

and

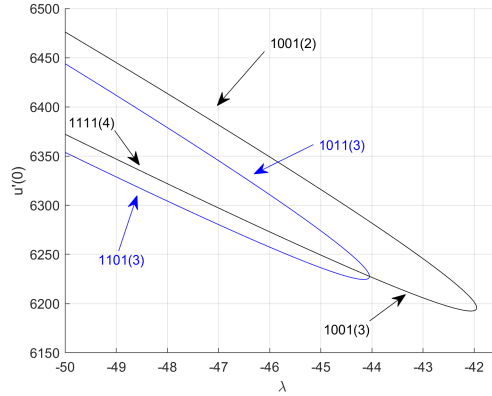
$$D_2 = -2 \int_0^1 w_1(x) \sin(7\pi x) \sin^2(\pi x) dx = \frac{1}{128\pi^2} > 0,$$

the component  $\mathcal{C}^+$  bifurcates supercritically from  $u = 0$  at  $\lambda = \pi^2$ , and exhibits a secondary bifurcation at  $\lambda_s \approx -2.85$ . It has been plotted in Figure 6a, which shows a significant piece of the global bifurcation diagram of the positive solutions of (1.1).



(A) Small positive solutions.

(B) Large positive solutions.



(C) A magnification of Figure 6b.

FIGURE 6. Scattered bifurcation diagrams for  $a(x) = \sin(7\pi x)$ .

Figure 6 consists of Figures 6a, 6b and 6c, where we are plotting, separately, the most significant branches of positive solutions that we have computed in our numerical experiments. By simply looking at the ordinate axis in Figures 6a and 6b, it is easily realized the ultimate reason why we are plotting these components in two separate figures. Whereas for those plotted on the left  $u'(0) < 3 \cdot 10^2$ , for those plotted on the right we have that  $u'(0) > 59 \cdot 10^2$ . So, plotting them in the same global bifurcation diagram would have pushed down against the  $\lambda$ -axis all the branches on the left, much like in Figure 4, but straightening this pushing effect. Figure 6c shows a zoom of the secondary bifurcation arising in Figure 6b, to detail the types of the positive solutions around it.

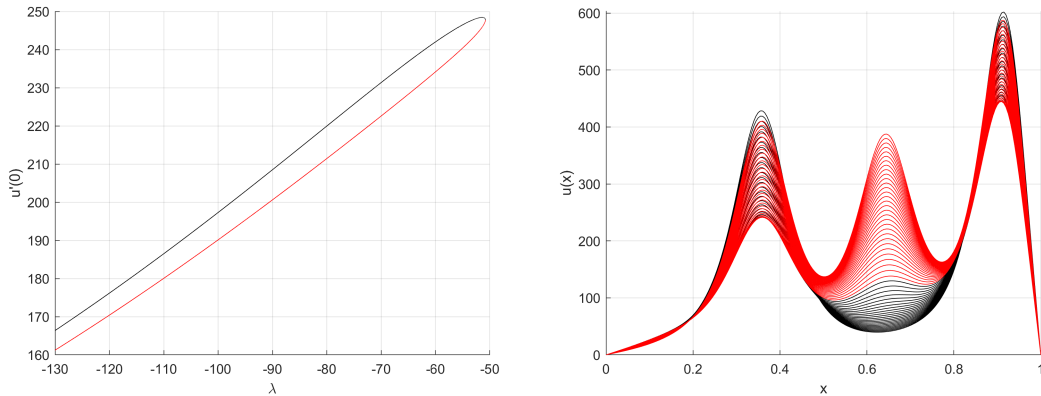
Since  $\mathcal{C}^+$  bifurcates from  $u = 0$  supercritically, by the exchange stability principle, [16], its solutions have Morse index zero until they reach the turning point. The bifurcation is very vertical in this case, hence, it is hard to determine for which  $\lambda$  the turning point occurs.

Anyway, Morse index increases to one as we pass the turning point and it remains the same until we reach the bifurcation point at  $\lambda_s \approx -2.85$ , where the Morse index becomes two for any smaller value of  $\lambda$ . By Theorem 2.1, the solutions  $(\lambda, u) \in \mathcal{C}^+$  with  $\lambda \approx \pi^2$  have the form  $s(\sin(\pi x) + y(s))$  for some  $s > 0$ ,  $s \approx 0$ . Thus, they have a single peak around 0.5. Once crossed  $\lambda_s$ , these solutions are of type 0110(2). The solutions along the bifurcated branches have types 0100(1) and 0010(1), respectively. So, this piece of the global bifurcation diagram seems to be generated by the two internal positive bumps of the weight function  $a(x)$ . Besides the component  $\mathcal{C}^+$ , Figure 6a shows two additional global subcritical folds. The solutions on the lower half-branch of the inferior folding have type 0001(1) and change to type 0011(2) on its upper half-branch, as the turning point of this component is crossed. Similarly, the solutions on the lower half-branch of the superior folding have type 0111(3) and change to type 0101(2) on the upper one. All those solutions can be generated, very easily, by taking into account that its type must begin with a 0, because  $u'(0)$  is small, while the remaining three digits should cover all the possible combinations of three elements taken from  $\{0, 1\}$ . Thus, counting  $u = 0$ , we have a total of  $2^3 = 8$  solutions for sufficiently negative  $\lambda$ .

Analogously, Figure 6b shows all solutions with  $u'(0)$  sufficiently large, whose types must begin with 1. Thus, it also shows a total of  $2^3 = 8$  solutions. According to our numerical experiments, these solutions are distributed into three components. Namely, two isolated global subcritical folds, plus a third component consisting of two interlaced subcritical folds, which is the component magnified and plotted in Figure 6c. The bifurcation along this component occurs at  $\lambda_s \approx -44.05$ .

According to these findings, based on a series of rather systematic numerical experiments, the sum of the four digits of the type of the solutions, i.e., their number of peaks, always provide us with the dimensions of their unstable manifolds, except for the solutions in a right neighborhood of the two bifurcation points on Figures 6a and 6c, where the solutions have types 0000(1) and 1001(3), respectively. Nevertheless, for sufficiently negative  $\lambda$ , this is a general rule.

In Figure 7 we have plotted a series of solutions of types 0111 and 0101 along the superior



(A) The blue upper fold of Figure 6a.

(B) Plots of solutions of type 0111(3) (red) and 0101(2) (black) on the branch plotted on the left.

FIGURE 7. Plots of solutions (right) along the branch (left) from Figure 6a.

fold (blue branch) of Figure 6a. The solutions on the lower half-branch are of type 0111, because they exhibit three peaks, and have been plotted in Figure 7b using red color. As the turning point is approached, the peaks of these solutions decrease until the central one is

almost glued as the turning point is crossed. Once switched the turning point, the solutions need some additional, very short, room for becoming of type 0101 pure, since the central peak still persists for a while, as it is illustrated in Figure 7b, where those solutions have been plotted in black color. Essentially, as the turning point is switched, the external peaks of the 0111 solutions increase, while the central peak is glued.

## 7. THE CASE $n = 2$ WITH AN ADDITIONAL PARAMETER $\mu$

In this section, we make the following choice

$$a(x) := \begin{cases} \mu \sin(5\pi x) & \text{if } x \in [0, 0.2) \cup (0.8, 1], \\ \sin(5\pi x) & \text{if } x \in [0.2, 0.8], \end{cases} \quad (7.1)$$

where  $\mu \geq 1$  is regarded as a secondary bifurcation parameter for (1.1). The behavior of this model for  $\mu = 1$  has been already described in Section 5. The bifurcation direction is

$$D_1 = -\frac{\sqrt{\frac{1}{2}(5 - \sqrt{5})} (5 - \sqrt{5})^2 (\mu - 1)}{128\pi} < 0$$

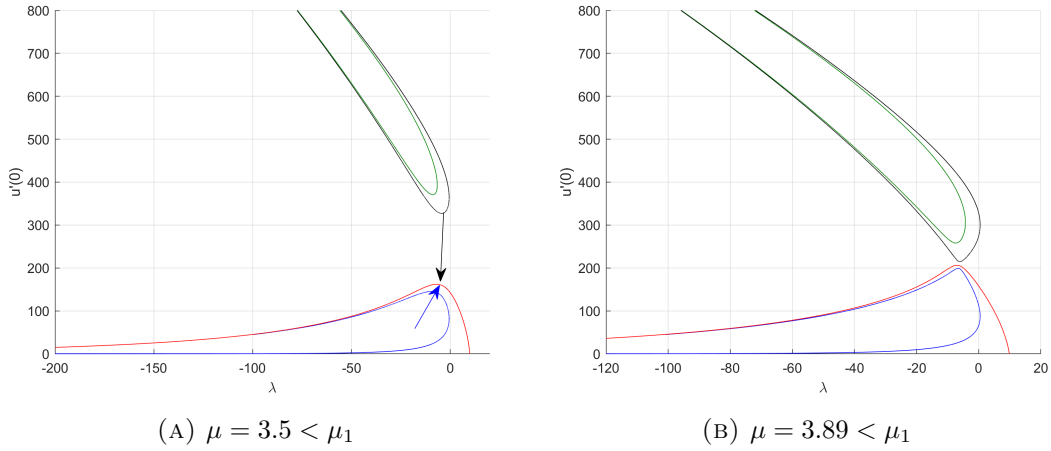
for all  $\mu > 1$  and hence, the bifurcation is always subcritical.

According to our numerical experiments, as we increase the value of  $\mu$ , the global bifurcation diagram remains very similar to the one plotted in Figures 4 and 5, up to reaching the critical value  $\mu_1 \approx 3.895$ , where the global structure of the bifurcation diagram changes. Figures 8a and 8b plot the corresponding global bifurcation diagram for  $\mu = 3.5$  and  $\mu = 3.89$ , respectively, whose global structure, topologically, coincides with the one already computed in Section 5 for  $\mu = 1$ .

Essentially, as  $\mu$  separates away from  $\mu = 1$  increasing towards  $\mu = \mu_1$ , the two subcritical folds lying in the upper part of the global bifurcation diagram plotted in Figure 4 are getting closer approaching the peak of the corresponding component  $\mathcal{C}^+ \equiv \mathcal{C}_\mu^+$ , as well as the global subcritical folding beneath, as sketched in Figure 8.

According to our numerical experiments, at the critical value of the parameter  $\mu_1$ , the set of positive solutions of (1.1) consists of two components, instead of four, because three of the previous four components of the problem for  $\mu < \mu_1$  are now touching at a single point playing the role of a sort of *organizing center* with respect to the secondary parameter  $\mu$ , whereas the upper interior supercritical folding remains separated away from  $\mathcal{C}_{\mu_1}^+$ . Naturally,  $\mathcal{C}_{\mu_1}^+$  consists of  $\lim_{\mu \uparrow \mu_1} \mathcal{C}_\mu^+$  plus the limits of the previous exterior upper folds and folds beneath  $\mathcal{C}_\mu^+$  for  $\mu < \mu_1$ .

The numerics suggests that, as  $\mu$  increases separating away from  $\mu_1$ , the touching point of the old three components spreads out into two secondary bifurcation points from the new component  $\mathcal{C}_\mu^+$ , in such a way that the “previous” folds do now bifurcate from  $\mathcal{C}_\mu^+$  at these two bifurcation values with respect to the primary parameter  $\lambda$ , say  $\lambda_1(\mu) > \lambda_2(\mu)$ , as illustrated in Figure 9a, where it becomes apparent how the old upper interior folding component still remains separated away from  $\mathcal{C}_\mu^+$ . Essentially, the upper half-branch of the old folding above  $\mathcal{C}_\mu^+$  together with the lower half-branch of the old interior folding provide us with the branch bifurcating from  $\mathcal{C}_\mu^+$  at  $\lambda_2(\mu)$ , for  $\mu > \mu_1$ , whereas the lower half-branch of the old folding above  $\mathcal{C}_\mu^+$  together with the upper half-branch of the old interior folding provide us with the new branch bifurcating from  $\mathcal{C}_\mu^+$  at  $\lambda_1(\mu)$ . And this situation persists for all  $\mu \in (\mu_1, \mu_2)$ , where  $\mu_2 \approx 3.925$ . The bigger is  $\mu$  in the interval  $(\mu_1, \mu_2)$ , the more separated stay the two bifurcation values  $\lambda_1(\mu)$  and  $\lambda_2(\mu)$  and the more approaches the exterior upper fold to the component  $\mathcal{C}_\mu^+$ . The separation between the bifurcation values is very well illustrated by the

FIGURE 8. Global bifurcation diagrams for  $\mu < \mu_1$ .

next table that provides us with the corresponding values of  $\lambda_1(\mu)$  and  $\lambda_2(\mu)$  for three values of  $\mu$  in  $(\mu_1, \mu_2)$ :

$\mu$	3.9	3.91	3.92
$\lambda_1(\mu)$	-5.1186	-4.4513	-3.9938
$\lambda_2(\mu)$	-7.5845	-8.4129	-9.0284

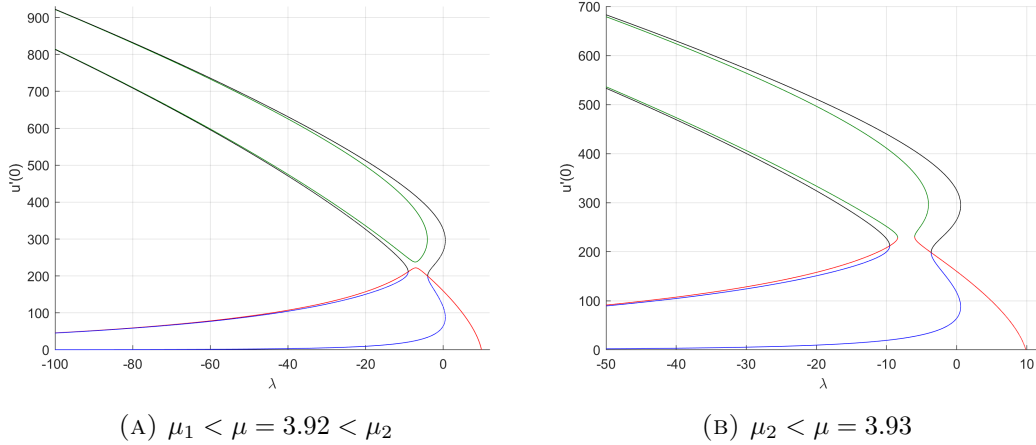
TABLE 1.  $\lambda_i(\mu)$  for three values of  $\mu \in (\mu_1, \mu_2)$ .

FIGURE 9. Two significant global bifurcation diagrams

And this situation persists, until  $\mu$  reaches the critical value  $\mu_2$ , where, according to the numerics, the exterior folding touches  $\mathcal{C}_{\mu_2}^+$  at a single point, in such a way that the set of positive solutions of (1.1) consists of the single component  $\mathcal{C}_{\mu_2}^+$ . As  $\mu > \mu_2$  separates away from  $\mu_2$ , our numerical experiments provide us with the global bifurcation diagram plotted in Figure 9b, where, once again, the set of positive solutions of (1.1) consists of two components,

$\mathcal{C}_\mu^+$  plus a global subcritical fold with a bifurcated secondary branch with the structure of a global subcritical folding. Thus, a new re-organization of the previous solution branches has occurred through a sort of mutual re-combination.

The global bifurcation diagrams remained topologically equivalent for all values of  $\mu > \mu_2$  for which we computed them. Figures 9b and 10a plot them for  $\mu = 3.93$  and  $\mu = 4.5$ , respectively. In both cases, the set of positive solutions consists of  $\mathcal{C}_\mu^+$  plus two global subcritical folds that meet at a single point, which can be viewed as a secondary bifurcation point from any of them. This structure persists for any further larger values of  $\mu$ . Figure 10b shows a magnification of the most significant parts of Figure 10a superimposing the individual types of the solutions together with the dimensions of their unstable manifolds.

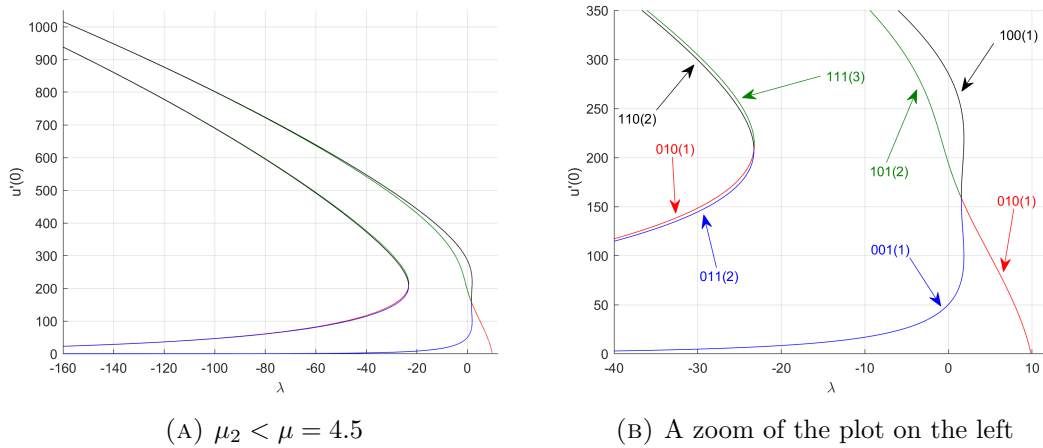


FIGURE 10. Global bifurcation diagram for  $\mu > \mu_2$

In full agreement with Conjecture 3.1, for every  $\mu \geq 1$ , there exists  $\lambda(\mu) < 0$  such that (1.1) has  $2^3 - 1 = 7$  positive solutions for every  $\lambda \leq \lambda(\mu)$ . For the choice  $\mu = 4.5$ ,  $\lambda(\mu) \approx -23.27$  equals the  $\lambda$ -coordinate of the bifurcation point of the global subcritical folds. Note that, for this special choice, (1.1) possesses three solutions at  $\lambda = 0$ .

Figure 11 plots a series of solutions with types 100 and 001 along the blue/black branch of Figure 10b that is part of the component  $\mathcal{C}_\mu^+$ , which has been isolated in Figure 11a. According to our numerical experiments, the solutions on the lower half-branch are of type 001; they have been plotted using red color. As the branching point is approached (see Figure 10b), the right peak diminishes and the solution looks like the first eigenfunction  $\sin(\pi x)$ . At the branching point, the solution changes its old type to 100. These solutions have been plotted using black color. The peak on the left starts to increase as we separate away from the bifurcation value.

## 8. NUMERICS OF BIFURCATION PROBLEMS

To discretize (1.1) we have used two methods. To compute the small positive solutions bifurcating from  $u = 0$  we implemented a pseudo-spectral method combining a trigonometric spectral method with collocation at equidistant points, as in R. Gómez-Reñasco and J. López-Gómez [28, 31], J. López-Gómez, J. C. Eilbeck, K. Duncan and M. Molina-Meyer [42], J. López-Gómez and M. Molina-Meyer [44, 45, 46], J. López-Gómez, M. Molina-Meyer and A. Tellini [47], J. López-Gómez, M. Molina-Meyer and P. H. Rabinowitz [48], and M. Fencl and J. López-Gómez [25]. This gives high accuracy at a rather reasonable computational cost (see,

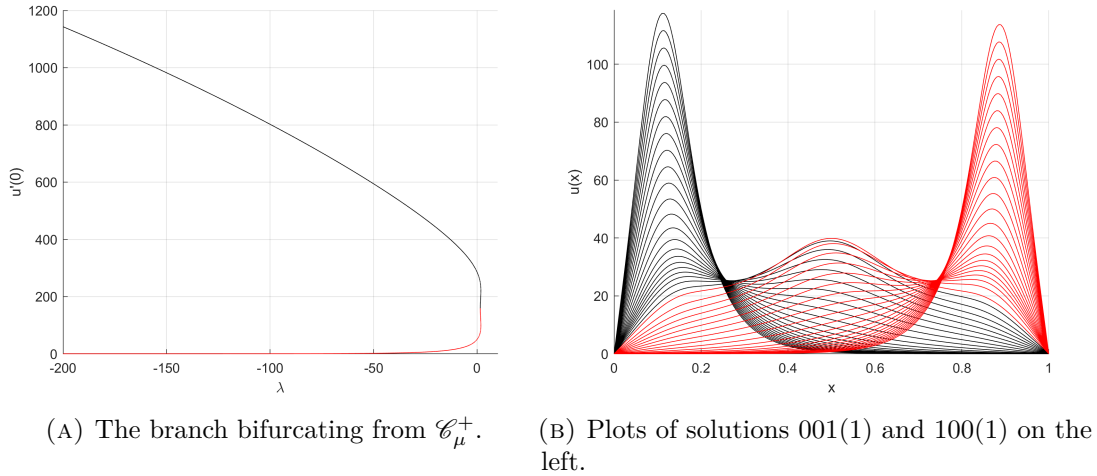


FIGURE 11. Plots of solutions (right) along the branch (left) from Figure 10a.

e.g., Canuto, Hussaini, Quarteroni and Zang [13]). However, to compute the large positive solutions we have preferred a centered finite differences scheme, which gives high accuracy at a lower computational cost, as it runs much faster in computing global solution branches in the bifurcation diagrams.

The pseudo-spectral method is more efficient and versatile for choosing the shooting direction from the trivial solution in order to compute the small positive solution of  $\mathcal{C}^+$ , as well as to detect the bifurcation points along the solution branches. Its main advantage in accomplishing this task comes from the fact that it provides us with the true bifurcation values from the trivial solution, while the scheme in differences only gives a rough approximation to these values. A pioneering reference on these methods is the paper of J. C. Eilbeck [22], which was seminal for the research teams of the second author.

For computing all the global subcritical folds arisen along this paper, we adopted the following, rather novel, methodology. Once computed  $\mathcal{C}^+$ , including all bifurcating branches from the primary curve emanating from  $u = 0$  at  $\lambda = \pi^2$ , one can ascertain the types of the solutions in  $\mathcal{C}^+$  for sufficiently negative  $\lambda$ . As, due to Conjecture 3.1 and the argument supporting it in Section 1, we already know that (1.1) admits  $2^{n+1} - 1$  positive solutions for sufficiently negative  $\lambda$ , together with their respective types, we can determine the types of all solutions of (1.1) for  $\lambda$  sufficiently negative that remained outside the component  $\mathcal{C}^+$ . Suppose, e.g., that we wish to compute the solution curve containing the positive solutions of type 011(2) in Figure 10b. Then, we consider as the initial iterate,  $u_0$ , for the underlying Newton method some function with a similar shape. If the choice is sufficiently accurate, after finitely many iterates, whose number depends on how far away stays from the true solution the initialization  $u_0$ , the Newton scheme should provide us with the first positive solution on that particular component. Once located the first point, our numerical path-following codes provide us with the entire solution curve almost algorithmically though the code developed by H. B. Keller and Z. H. Yang [33] to treat the turning points of these folds as if they were regular points treated with the implicit function theorem.

The huge complexity of some of the computed bifurcation diagrams, as well as their deepest quantitative features, required an extremely careful control of all the steps in the involved subroutines. This explains why the available commercial bifurcation solver packages, such

as AUTO-07P, are almost un-useful to deal with differential equations, like the one of (1.1), with heterogeneous coefficients. As noted by E. J. Doedel and B. E. Oldeman in [21, p.18],

*“given the non-adaptive spatial discretization, the computational procedure here is not appropriate for PDEs with solutions that rapidly vary in space, and care must be taken to recognize spurious solutions and bifurcations.”*

This is nothing than one of the main problems that we found in our numerical experiments, as the number of critical points of the solutions increases according to the dimensions of their unstable manifolds, and the solutions grew up to infinity as  $\lambda \downarrow -\infty$  within the intervals of  $\text{supp } a^+$ , while, due to Theorem 3.1, they decayed to zero on the intervals where  $a(x)$  is negative. Naturally, for all numerical methods is a serious challenge to compute solutions exhibiting simultaneously internal and boundary layers, where the gradients can oscillate as much as wish for sufficiently negative  $\lambda$ .

For general Galerkin approximations, the local convergence of the solution paths at regular, turning and simple bifurcation points was proven by F. Brezzi, J. Rappaz and P. A. Raviart in [8, 9, 10] and by J. López-Gómez, M. Molina-Meyer and M. Villareal [49] and J. López-Gómez, J. C. Eilbeck, K. Duncan and M. Molina-Meyer in [42] for codimension two singularities in the context of systems. In these situations, the local structure of the solution sets for the continuous and the discrete models are known to be equivalent.

The global continuation solvers used to compute the solution curves of this paper, as well as the dimensions of the unstable manifolds of all the solutions filling them, have been built from the theory on continuation methods of E. L. Allgower and K. Georg [2], M. Crouzeix and J. Rappaz [17], J. C. Eilbeck [22], H. B. Keller [32], J. López-Gómez [36] and J. López-Gómez, J. C. Eilbeck, K. Duncan and M. Molina-Meyer [42].

## 9. FINAL DISCUSSION

Our systematic numerical experiments have confirmed that the following features should be true for a general  $a(x)$  such that  $\text{supp } a^+$  consists of  $n + 1$  intervals separated away by  $n$  intervals where  $a$  is negative:

- For sufficiently negative  $\lambda$ , (1.1) has, at least,  $2^{n+1} - 1$  positive solutions. Actually, for the special choice (1.2), it should have exactly  $2^{n+1} - 1$ . This strengthens Conjecture 3.1, going back to [28], which has been shown to be true when  $a(x)$  is symmetric and piece-wise constant on the support of  $a^+$ .
- For sufficiently negative  $\lambda$ , the Morse index of any positive solution  $u$  of type  $d_1 d_2 \cdots d_{n+1}$ ,  $d_j \in \{0, 1\}$ , is given by

$$\mathcal{M}(u) := \sum_{j=1}^{n+1} d_j.$$

- The eventual symmetric character of the solutions cannot be lost along any of the computed components, unless a branching point is crossed. Thus, each fold consists of either symmetric solutions around 0.5, or asymmetric ones.

Note that in the special case when  $a(x)$  is given by (1.2),  $a(0.5) < 0$  if  $n$  is odd, while  $a(0.5) > 0$  if  $n$  is even. Moreover, according to our numerical experiments, the component  $\mathcal{C}^+$  does not admit any branching point if  $n = 2$ , whereas it admits one if  $n \in \{1, 3\}$ . Thus, one might be tempted to believe that, in general,  $\mathcal{C}^+$  should not have any branching point if

$a(0.5) < 0$ . Our numerical experiments in Section 7 show that, for the special choice

$$a(x) := \begin{cases} 4.5 \sin(5\pi x) & \text{if } x \in [0, 0.2) \cup (0.8, 1], \\ \sin(5\pi x) & \text{if } x \in [0.2, 0.8], \end{cases} \quad (9.1)$$

the component  $\mathcal{C}^+$  has a branching point (see Figure 10b), though  $a(0.5) < 0$ . Thus, one should be extremely careful in conjecturing anything from either numerical experiments, or heuristical considerations in population dynamics, as they might drive experts to make wrong conjectures, as the one originating the counterexample of E. Sovrano [62].

According to the numeric of Section 7, the problem

$$\begin{cases} -u'' = a(x)u^2 & \text{in } (0, 1), \\ u(0) = u(1) = 0, \end{cases} \quad (9.2)$$

for the special choice (9.1) has, exactly, three positive solutions, and it should not admit anymore, to be consistent the number of solutions with the global structure of the bifurcation diagram (see Figure 10b). Thus, Corollary 1.4.2 of G. Feltrin [23] is optimal in the sense that it cannot be satisfied for sufficiently small  $\mu > 0$ . Most precisely, does not hold when  $\mu = 1$  for the special choice (9.2). Since (1.1) still possesses  $2^3 - 1 = 7$  positive solutions for sufficiently negative  $\lambda < 0$ , this example also shows the independence between Conjecture 3.1 and the multiplicity results of G. Feltrin and F. Zanolin [24] and G. Feltrin [23].

For every  $\mu \in (3.895, 3.925)$ , the component  $\mathcal{C}^+$  of (1.1) for the special choice

$$a(x) := \begin{cases} \mu \sin(5\pi x) & \text{if } x \in [0, 0.2) \cup (0.8, 1], \\ \sin(5\pi x) & \text{if } x \in [0.2, 0.8], \end{cases} \quad (9.3)$$

exhibits two bifurcation points along it. This might be the first example of this nature documented in the abundant literature on superlinear indefinite problems.

As, generically, higher order bifurcations break down by the eventual asymmetries of the weight functions, as discussed in Chapter 7 of [38] and in [55], we conjecture that

- Generically, when  $a(x)$  is asymmetric about 0.5, the set of positive solutions of (1.1) consists of the component  $\mathcal{C}^+$  plus  $n$  supercritical folds,  $\mathcal{D}_j$ ,  $j \in \{1, \dots, n\}$ , in such a way that, for sufficiently negative  $\lambda < 0$ , (1.1) admits, at least, one solution in  $\mathcal{C}^+$  and two solutions in  $\mathcal{D}_j$  for each  $j \in \{1, \dots, n\}$ .

The global bifurcation diagram plotted in Figure 5 being a paradigm of this global topological behavior.

The analysis of the reorganization in components of the positive solutions of (1.1) carried out in Section 7 for the special choice (9.3) when  $\mu$  increases from 3.89 up to reach the value  $\mu = 3.93$  reveals the high complexity that the global bifurcation diagrams of (1.1) might have when  $a(x)$  changes of sign a large number of times by incorporating the appropriate control parameters into the problem. Getting any insight into this problem seems an extremely serious challenge.

## REFERENCES

- [1] S. Alama and G. Tarantello, Elliptic problems with nonlinearities indefinite in sign, *J. Funct. Anal.* **141** (1996), 159–215.
- [2] E. L. Allgower and K. Georg, *Introduction to Numerical Continuation Methods*, SIAM Classics in Applied Mathematics 45, SIAM, Philadelphia, 2003.
- [3] H. Amann and J. López-Gómez, A priori bounds and multiple solutions for superlinear indefinite elliptic problems, *J. Diff. Eqns.* **146** (1998), 336–374.
- [4] A. Ambrosetti, M. Badiale and S. Cingolani, Semiclassical states of nonlinear Schrödinger equations, *Arch. Rat. Mech. Anal.* **140** (1997), 285–300.

- [5] H. Berestycki, I. Capuzzo-Dolcetta and L. Nirenberg, Superlinear indefinite elliptic problems and nonlinear Liouville theorems, *Topol. Methods Nonl. Anal.* **4** (1994) 59–78.
- [6] H. Berestycki, I. Capuzzo-Dolcetta and L. Nirenberg, Variational methods for indefinite superlinear homogeneous elliptic problems, *Nonl. Diff. Eqns. Appl.* **2** (1995), 553–572.
- [7] H. Berestycki and P. L. Lions, Some applications of the method of super and subsolutions, in *Bifurcation and nonlinear eigenvalue problems* (Proc., Session, Univ. Paris XIII, Villetaneuse, 1978), pp. 16–41, Lecture Notes in Mathematics 782, Springer, Berlin, 1980.
- [8] F. Brezzi, J. Rappaz and P. A. Raviart, Finite dimensional approximation of nonlinear problems, part I: Branches of nonsingular solutions, *Numer. Math.* **36** (1980), 1–25.
- [9] F. Brezzi, J. Rappaz and P. A. Raviart, Finite dimensional approximation of nonlinear problems, part II: Limit points, *Numer. Math.* **37** (1981), 1–28.
- [10] F. Brezzi, J. Rappaz and P. A. Raviart, Finite dimensional approximation of nonlinear problems, part III: Simple bifurcation points, *Numer. Math.* **38** (1981), 1–30.
- [11] G. Buttazzo, M. Giaquinta and S. Hildebrandt, *One-dimensional Variational Problems*, Clarendon Press, Oxford, 1998.
- [12] S. Cano-Casanova and J. López-Gómez, Properties of the principal eigenvalues of a general class of nonclassical mixed boundary value problems, *J. Dif. Eqns.* **178** (2002), 123–211.
- [13] C. Canuto, M. Y. Hussaini, A. Quarteroni and T. A. Zang, *Spectral Methods in Fluid Mechanics*, Springer, Berlin, Germany, 1988.
- [14] S. Cingolani and M. Lazzo, Multiple positive solutions to nonlinear Schrödinger equations with competing potential functions, *J. Diff. Eqns.* **160** (2000), 118–138.
- [15] M. G. Crandall and P. H. Rabinowitz, Bifurcation from simple eigenvalues, *J. Funct. Anal.* **8** (1971), 321–340.
- [16] M. G. Crandall and P. H. Rabinowitz, Bifurcation, perturbation of simple eigenvalues and linearized stability, *Arch. Rat. Mech. Anal.* **52** (1973), 161–180.
- [17] M. Crouzeix and J. Rappaz, *On Numerical Approximation in Bifurcation Theory*, Recherches en Mathématiques Appliquées 13, Masson, Paris, 1990.
- [18] E. N. Dancer and J. Wei, On the effect of domain topology in a singular perturbation problem, *Top. Meth. Nonl. Anal.* **11** (1998), 227–248.
- [19] M. del Pino and P. Felmer, Semi-classical states for nonlinear Schrödinger equations, *J. Funct. Anal.* **149** (1997), 245–265.
- [20] M. del Pino and P. Felmer, Multipeak bound states for nonlinear Schrödinger equations, *Ann. Inst. Henri Poincaré* **15** (1998), 127–149.
- [21] E. J. Doedel and B. E. Oldeman, AUTO-07P: Continuation and bifurcation software for ODEs, 2012, <http://www.dam.brown.edu/people/sandsted/auto/auto07p.pdf>.
- [22] J. C. Eilbeck, The pseudo-spectral method and path-following in reaction-diffusion bifurcation studies, *SIAM J. Sci. Stat. Comput.* **7** (1986), 599–610.
- [23] G. Feltrin, *Positive Solutions to Indefinite Problems, A Topological Approach*, Frontiers in Mathematics, Birkhäuser, 2018.
- [24] G. Feltrin and F. Zanolin, Multiple positive solutions for a superlinear problem: a topological approach, *J. Diff. Equ.* **259** (2015), 925–963.
- [25] M. Fencl and J. López-Gómez, Nodal solutions of weighted indefinite problems, *submitted*.
- [26] S. Fernández-Rincón and J. López-Gómez, The Picone identity: A device to get optimal uniqueness results and global dynamics in Population Dynamics, arXiv:1911.05066v2 [math.AP] 20 Nov 2019.
- [27] M. Gaudenzi, P. Habets and F. Zanolin, A seven-positive-solutions theorem for a superlinear problem, *Adv. Nonlinear Stud.* **4** (2004), 149–164.
- [28] R. Gómez-Reñasco and J. López-Gómez, The effect of varying coefficients on the dynamics of a class of superlinear indefinite reaction diffusion equations, *J. Diff. Eqns.* **167** (2000), 36–72.
- [29] R. Gómez-Reñasco and J. López-Gómez, The uniqueness of the stable positive solution for a class of superlinear indefinite reaction diffusion equations, *Diff. Int. Eqns.* **14** (2001), 751–768.
- [30] R. Gómez-Reñasco and J. López-Gómez, The effect of varying coefficients on the dynamics of a class of superlinear indefinite reaction diffusion arising in population dynamics, unpublished preprint 1999. Numerical experiments incorporated to Chapter 9 of [41].
- [31] R. Gómez-Reñasco and J. López-Gómez, On the existence and numerical computation of classical and non-classical solutions for a family of elliptic boundary value problems, *Nonl. Anal. TMA* **48** (2002), 567–605.

- [32] H. B. Keller, *Lectures on Numerical Methods in Bifurcation Problems*, Tata Institute of Fundamental Research, Springer, Berlin, Germany, 1986.
- [33] H. B. Keller and Z. H. Yang, A direct method for computing higher order folds, *SIAM J. Sci. Stat.* **7** (1986), 351–361.
- [34] M. Langlais and D. Phillips, Stabilization of solutions of nonlinear and degenerate evolution equations, *Nonlinear Anal.* **9** (1985), 321–333.
- [35] Y. Le, J. Wei and H. Xu, Multi-bump solutions of  $-\Delta u = K(x)u^{\frac{n+2}{n-2}}$  on lattices in  $\mathbb{R}^n$ , *J. reine angew. Math.* **743** (2018), 163–211.
- [36] J. López-Gómez *Estabilidad y Bifurcación Estática. Aplicaciones y Métodos Numéricos*, Cuadernos de Matemática y Mecánica, Serie Cursos y Seminarios 4, Santa Fe, R. Argentina, 1988.
- [37] J. López-Gómez, Varying bifurcation diagrams of positive solutions for a class of superlinear indefinite boundary value problems, *Trans. Amer. Math. Soc.* **352** (2000), 1825–1858.
- [38] J. López-Gómez, *Spectral Theory and Nonlinear Functional Analysis*, CRC Press, Boca Raton, 2001.
- [39] J. López-Gómez, Uniqueness of radially symmetric large solutions, *Disc. Cont. Dyn. Systems Supplement* (2007), 677–686.
- [40] J. López-Gómez, *Linear Second Order Elliptic Operators*, World Scientific Publishing, 2013.
- [41] J. López-Gómez, *Metasolutions of Parabolic Equations in Population Dynamics*, CRC Press, Boca Raton, 2016.
- [42] J. López-Gómez, J. C. Eilbeck, K. Duncan and M. Molina-Meyer, Structure of solution manifolds in a strongly coupled elliptic system, *IMA J. Numer. Anal.* **12** (1992), 405–428.
- [43] J. López-Gómez and M. Molina-Meyer, Bounded components of positive solutions of abstract fixed point equations: mushrooms, loops and isolas, *J. Diff. Eqns.* **209** (2005), 416–441.
- [44] J. López-Gómez and M. Molina-Meyer, Superlinear indefinite systems: Beyond Lotka Volterra models, *J. Differ. Eqns.* **221** (2006), 343–411.
- [45] J. López-Gómez and M. Molina-Meyer, The competitive exclusion principle versus biodiversity through segregation and further adaptation to spatial heterogeneities, *Theor. Popul. Biol.* **69** (2006), 94–109.
- [46] J. López-Gómez and M. Molina-Meyer, Modeling coepetition, *Math. Comput. Simul.* **76** (2007), 132–140.
- [47] J. López-Gómez, M. Molina-Meyer and A. Tellini, Intricate dynamics caused by facilitation in competitive environments within polluted habitat patches, *Eur. J. Appl. Maths.* doi:10.1017/S0956792513000429 (2014), 1–17.
- [48] J. López-Gómez, M. Molina-Meyer and P. H. Rabinowitz, Global bifurcation diagrams of one node solutions in a class of degenerate boundary value problems, *Disc. Cont. Dyn. Sys. B* **22** (2017), 923–946.
- [49] J. López-Gómez, M. Molina-Meyer and M. Villareal, Numerical coexistence of coexistence states, *SIAM J. Numer. Anal.* **29** (1992), 1074–1092.
- [50] J. López-Gómez and P. Omari, Global components of positive bounded variation solutions of a one-dimensional indefinite quasilinear Neumann problem, *Adv. Nonlinear Stud.* **19** (2019) 437–473.
- [51] J. López-Gómez and P. Omari, Characterizing the formation of singularities in a superlinear indefinite problem related to the mean curvature operator, *J. Differ. Equ.* **269** (2020), 1544–1570.
- [52] J. López-Gómez and P. Omari, Regular versus singular solutions in a quasilinear indefinite problem with an asymptotically linear potential, *Adv. Nonlinear Stud.* <https://doi.org/10.1515/ans-2020-2083>.
- [53] J. López-Gómez, P. Omari, S. Rivetti, Positive solutions of one-dimensional indefinite capillarity-type problems, *J. Differ. Equ.* **262** (2017) 2335–2392.
- [54] J. López-Gómez, P. Omari and S. Rivetti, Bifurcation of positive solutions for a one-dimensional indefinite quasilinear Neumann problem, *Nonlinear Anal.* **155** (2017) 1–51.
- [55] J. López-Gómez and A. Tellini, Generating an arbitrarily large number of isolas in a superlinear indefinite problem, *Nonl. Anal.* **108** (2014), 223–248.
- [56] J. López-Gómez, A. Tellini and F. Zanolin, High multiplicity and complexity of the bifurcation diagrams of large solutions for a class of superlinear indefinite problems, *Commun. Pure Appl. Anal.* **13** (2014), 1–73.
- [57] H. Matano, Nonincrease of the lap-number of a solution for a one-dimensional semilinear parabolic equation, *J. Fac. Sci. Univ. Tokyo Sect. IA Math.* **29** (1982), 401–441.
- [58] L. Nirenberg, A strong maximum principle for parabolic equations, *Comm. Pure Appl. Maths.* **6** (1953), 167–177.
- [59] J. Mawhin, D. Papini and F. Zanolin, Boundary blow-up for differential equations with indefinite weight, *J. Diff. Eqns.* **188** (2003), 33–51.
- [60] P. H. Rabinowitz, Some global results for nonlinear eigenvalue problems, *J. Funct. Anal.* **7** (1971), 487–513.

- [61] D. H. Sattinger, *Topics in stability and bifurcation theory*, Lecture Notes in Mathematics, Vol. 309. Springer-Verlag, Berlin–New York, 1973.
- [62] E. Sovrano, A negative answer to a conjecture arising in the study of selection-migration models in population genetics, *J. Math. Biol.* **76** (2018), 1655–1672.
- [63] J. Wei, On the construction of single-peaked solutions to a singularly perturbed semilinear Dirichlet problem, *J. Diff. Eqns.* **129** (1996), 315–333.

DEPARTMENT OF MATHEMATICS AND NTIS, FACULTY OF APPLIED SCIENCES, UNIVERSITY OF WEST BOHEMIA, UNIVERZITNÍ 8, 30100, PLZEN, CZECH REPUBLIC  
*E-mail address:* `fenc1m37@ntis.zcu.cz`

INSTITUTE OF INTER-DISCIPLINAR MATHEMATICS (IMI) AND DEPARTMENT OF ANALYSIS AND APPLIED MATHEMATICS, COMPLUTENSE UNIVERSITY OF MADRID, MADRID 28040, SPAIN  
*E-mail address:* `Lopez_Gomez@mat.ucm.es`